Numerical Solution of the Beltrami Equation Via a Purely Linear System

R. Michael Porter & Hirokazu Shimauchi

Constructive Approximation

ISSN 0176-4276

Constr Approx
DOI 10.1007/s00365-016-9334-6

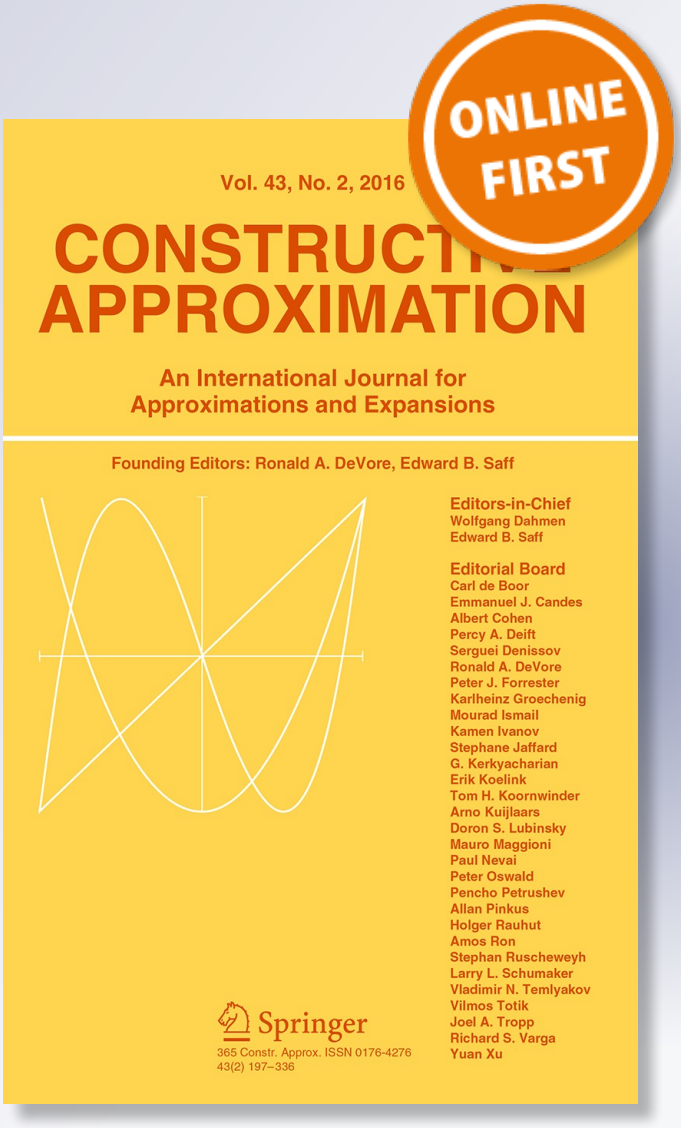

Springer

Constr Approx
DOI 10.1007/s00365-016-9334-6

CONSTRUCTIVE
APPROXIMATION

Numerical Solution of the Beltrami Equation Via a Purely Linear System

R. Michael Porter[1] · **Hirokazu Shimauchi**[2]

Received: 1 July 2014 / Revised: 3 January 2016 / Accepted: 11 February 2016

Abstract An effective algorithm is presented for solving the Beltrami equation $\partial f/\partial \overline{z} = \mu\, \partial f/\partial z$ in a planar disk. The disk is triangulated in a simple way, and f is approximated by piecewise linear mappings; the images of the vertices of the triangles are defined by an overdetermined system of linear equations. (Certain apparently nonlinear conditions on the boundary are eliminated by means of a symmetry construction.) The linear system is sparse, and its solution is obtained by standard least-squares, so the algorithm involves no evaluation of singular integrals nor any iterative procedure for obtaining a single approximation of f. Numerical examples are provided, including a deformation in a Teichmüller space of a Fuchsian group.

Keywords Numerical quasiconformal mapping · Numerical conformal mapping · Beltrami equation · Quadratic differential · Triangular mesh

Mathematics Subject Classification 30C62

Communicated by Stephan Ruscheweyh.

The first author was partially supported by CONACyT Grant 166183. The second author was supported by International Advanced Research and Education Organization in Tohoku University.

✉ R. Michael Porter
mike@math.cinvestav.edu.mx

Hirokazu Shimauchi
shimauchi@ims.is.tohoku.ac.jp; hirokazu.shimauchi@gmail.com

[1] Department of Mathematics, Centro de Investigación y de Estudios Avanzados del I.P.N., Apdo. Postal 1-798, Arteaga 5, 76000 Querétaro, QRO, Mexico

[2] Division of Mathematics, Graduate School of Information Sciences, Tohoku University, 6-3-09 Aramaki-Aza-Aoba, Aoba-ku, Sendai 980-8579, Japan

Published online: 18 April 2016

1 Introduction

The Beltrami equation

$$\frac{\partial f(z)/\partial \overline{z}}{\partial f(z)/\partial z} = \mu(z) \tag{1}$$

determines a unique normalized quasiconformal self-mapping f of the unit disk $\mathbb{D} = \{z\colon\ |z| < 1\}$ in the complex plane. Here μ is a given measurable function in $\mathbb{D}$ with $\|\mu\|_\infty < 1$ and is called the Beltrami derivative (or complex dilatation) of f. One says that f is μ-conformal.

The Beltrami equation has been the object of deep investigation, in large measure due to its importance in the theory of deformations of Kleinian groups and their applications to Teichmüller spaces [13,17]. Other applications of the Beltrami equation as mentioned in the introduction to [7] are quite well known, and we will not go into them here. Some more recent applications, such as mapping of the cerebral cortex, use the Beltrami equation in the spirit of its original application, dating back to Gauss, for finding a conformal mapping from a surface in 3-space onto a planar region; this is done effectively in [2] although without explicit use of the Beltrami derivative μ. The Beltrami derivative has also been proposed as a way of compressing data for surface maps [20], and is an essential element of the solution of the conductivity equation in [3] and solution of subsonic flow problems in [8].

With this increasing use of computer applications, it has become of great interest to know how solve the Beltrami equation numerically. One method for doing this is suggested naturally by the classical existence proof given by Mori–Boyarskii–Ahlfors–Bers [13,17]. For this method, one must evaluate singular integrals of the form

$$T_m g(z) = -\frac{1}{\pi} \iint_{\mathbb{D}} \frac{g(\zeta)}{(\zeta - z)^m}\, \mathrm{d}\xi \mathrm{d}\eta, \quad m = 1, 2$$

(defined as Cauchy principal values when $m = 2$), and then calculate sums of Neumann series of the form $\sum T_2(\mu T_2(\cdots(\mu T_2(\mu)\cdots))$. A related approach involving the singular integrals was developed by Daripa and Mashat [6,7], and refined by Gaidashev and Khmelev [11]. Instead of summing the Neumann series, their method involves iteration towards a solution of a related Dirichlet problem. Their work incudes refinement of the technique of evaluation of the singular integrals via FFT, which is of interest in itself.

He [14] proposed an alternative method of solving the Beltrami equation using circle packings. Williams [28] presented another circle-packing method, based on the idea of conformal welding. Little information is available on the numerical performance of these methods. Lui et al. [21] describe yet another method, which reduces the question of solving the Beltrami equation to that of a linear system on the underlying mesh. Their method, focused on obtaining Teichmüller mappings of prescribed domains (rather than self-mappings of a disk as we consider here), is applied to problems of face recognition and brain mapping. Many other approaches have been given to solve for quasiconformal mappings, often from surfaces in $\mathbb{R}^3$ to the plane. Descriptions and further references may be found in [9,12,16,19,22,24]. An attempt to solve the numerical solution of the Beltrami equation by applying conformal mappings as an

intermediate step was made in [23]. However, this method was later found not to converge to the proper solution and appears not to be salvageable.

In this paper, we give a much simpler algorithm with full proof of convergence in the case of a smooth Beltrami derivative. (We believe that this smoothness condition is overly restrictive, as numerical experiments suggest.) In Sect. 2, we gather the basic facts we will need about quasiconformal mappings. In Sects. 3 and 4, we explain how to set up the linear system describing the Beltrami equation. In Sect. 5, the algorithm is specified, and the main theorem on the convergence of the algorithm is stated and proved. Several numerical examples are provided in Sect. 6, including a deformation of a Fuchsian group. In the closing comments, we examine the corresponding computational cost of this method and discuss some alternative approaches to solving the Beltrami equation.

2 Preliminaries

We state here the basic definitions and terminology, as well as some of the standard results we will need concerning quasiconformal mappings and the Beltrami equation.

2.1 Affine Linear Quasiconformal Mappings

In this section, μ, a, b are complex constants subject to $a \neq 0$, $|\mu| < 1$, and we consider the mappings

$$L_\mu(z) = \frac{z + \mu\bar{z}}{1 + \mu}, \tag{2}$$

$$H_{a,b}(z) = az + b, \tag{3}$$

for $z \in \mathbb{C}$. Thus L_μ is μ-conformal and real-linear, while $H_{a,b}$ is conformal and affine complex-linear. Note that L_μ is determined by its value at any single finite point other than its fixed points $z = 0$ and $z = 1$, while $H_{a,b}$ is determined by the images of any two points. All μ-conformal affine linear mappings are of the form $H_{a,b} \circ L_\mu$, and this decomposition is unique. We will use the following form of expressing affine linear mappings.

Proposition 2.1 *Given z_1, z_2 distinct and w_1, w_2 distinct, together with $|\mu| < 1$, there is a unique μ-conformal affine linear mapping $B = B_{\mu;\, z_1, z_2;\, w_1, w_2}$ that sends z_1 to w_1 and z_2 to w_2. This mapping is given explicitly by*

$$\begin{aligned} B(z) &= w_1 + \frac{w_2 - w_1}{L_\mu(z_2 - z_1)} L_\mu(z - z_1) \\ &= \frac{L_\mu(z_2 - z)}{L_\mu(z_2 - z_1)} w_1 + \frac{L_\mu(z_1 - z)}{L_\mu(z_1 - z_2)} w_2. \end{aligned}$$

The coefficients of w_1, w_2 in this last expression are never 0, 1, or ∞ when z_1, z_2, z are distinct. As we will be interested in mappings of triangles, the following facts will be useful.

Corollary 2.2 *There exists a μ-conformal affine linear map that sends z_1, z_2, z_3 to w_1, w_2, w_3, respectively, if and only if*

$$L_\mu(z_2 - z_3)\, w_1 + L_\mu(z_3 - z_1)\, w_2 + L_\mu(z_1 - z_2)\, w_3 = 0. \tag{4}$$

Corollary 2.3 *Given z_1, z_2, z_3 noncollinear and w_1, w_2, w_3 noncollinear, there is a unique affine linear mapping that sends z_i to w_i ($i = 1, 2, 3$). Its Beltrami derivative is equal to*

$$\mu = -\frac{(z_2 - z_1)(w_3 - w_1) - (z_3 - z_1)(w_2 - w_1)}{(\overline{z_2} - \overline{z_1})(w_3 - w_1) - (\overline{z_3} - \overline{z_1})(w_2 - w_1)}. \tag{5}$$

Proof The affine linear mapping is well defined because each of the pairs $(z_2 - z_1, z_3 - z_1)$, $(w_2 - w_1, w_3 - w_1)$ is linearly independent over the real numbers. To calculate the Beltrami derivative, substitute (2) into the formula of Corollary 2.2 and solve for μ. □

In applying Corollary 2.3, one normally would also require the z- and w-triangles to be like-oriented, to ensure that $|\mu| < 1$.

2.2 Closeness to Similarity

The affine-conformal mapping $H_{a,b}$ of (3) sends triangles to similar triangles. A Beltrami derivative (5) can be regarded as a measure of how much the (positively oriented) triangles with vertices z_1, z_2, z_3 and w_1, w_2, w_3 fail to be similar. Indeed, these two triangles may be carried by conformal mappings of the form $H_{a,b}$ to normalized triangles $(0, 1, v_0)$, $(0, 1, v)$, respectively, and in turn the first of these is sent to the second under the mapping L_μ where

$$\mu = -\frac{v - v_0}{v - \overline{v_0}}. \tag{6}$$

With v_0 fixed, the relation $v \leftrightarrow \mu$ from $\operatorname{Im} v > 0$ to $|\mu| < 1$ thus associates an element of the unit disk to each similarity class of oriented triangles, and we can use $|\mu|$ as a measure of the discrepancy from being similar to the original triangle. In this regard, we must note that the Beltrami derivative of the affine mapping from (z_1, z_2, z_3) to (w_1, w_2, w_3) is $e^{2i \arg(z_2 - z_1)}\mu$ (cf. Proposition 2.8 below), so the absolute value is not altered by the fact of normalizing to the triangle $(0, 1, v_0)$ with horizontal base.

Observe that the function $\mu \mapsto L_\mu(v_0)$ is a Möbius transformation. It sends the family of circles $|\mu| =$ constant to a family of nested circles which all enclose $v_0 = L_0(v_0)$. The equations $L_\mu(v_0) = 0$ and $L_\mu(v_0) = 1$ have respective solutions $\mu = v_0/\overline{v_0}$ and $\mu_0 = -(1 - v_0)/(1 - \overline{v_0})$, both of absolute value equal to 1. Therefore the unit circle $\{|\mu| = 1\}$ is sent by this Möbius transformation to a circle passing through both 0 and 1. Thus for any fixed real value $0 \le \mu_0 < 1$, the set $L_\mu(\{|\mu| \le \mu_0\})$ is a disk that does not contain 0 or 1. The following proposition follows from application of this fact to the three values $v_0 = e^{-i\pi/6},\ e^{i\pi/3},\ i$ in (6).

Proposition 2.4 *Let $0 \le \mu_0 < 1$. Then the quantity*

$$\delta_{\mu_0} = \inf \left\{ |L_\mu(z)|,\ |L_\mu(z) - 1|,\ \frac{1}{|L_\mu(z)|} :\ z \in \left\{ e^{-i\pi/6},\ e^{i\pi/3},\ i \right\},\ |\mu| < \mu_0 \right\}$$

is positive.

Corollary 2.5 *Let z_1, z_2, z_3 be an equilateral triangle with one vertical edge, and let $0 \le \mu_0 < 1$. Then for $|\mu| < \mu_0$, the ratio of any two coefficients in equation (4) is bounded above and below by $(\delta_{\mu_0})^2$.*

Proof The hypothesis implies that edge vectors $z_2 - z_1$, $z_3 - z_2$, and $z_1 - z_3$ are among the values $\pm ce^{i\pi/3}$, $\pm ce^{-i\pi/6}$, $\pm ci$ for a fixed $c > 0$, so the coefficients in (4) are bounded below by c/δ_{μ_0} and above by $c\delta_{\mu_0}$. □

2.3 Quasiconformal Mappings

The following well-known general properties of quasiconformal mappings [1,17,18] are fundamental to this work.

Proposition 2.6 *If μ is measurable in $\mathbb{D} = \{z \in \mathbb{C} : |z| < 1\}$ and satisfies $\|\mu\|_\infty < 1$, then there is a unique μ-conformal mapping $f : \mathbb{D} \to \mathbb{D}$ of the disk onto itself whose (unique) extension as a homeomorphism of the closed disk $\overline{\mathbb{D}}$ satisfies the normalization*

$$f(0) = 0, \quad f(1) = 1.$$

Proposition 2.7 *Let μ, μ_n $(n = 1, 2, \dots)$ be measurable functions in $\mathbb{D}$ with $\|\mu_n\|_\infty \le c < 1$, and suppose that $\mu_n \to \mu$ pointwise as $n \to \infty$. Let f, f_n be the normalized solutions of the corresponding Beltrami equations given by Proposition 2.6. Then f_n converge to f uniformly on $\overline{\mathbb{D}}$.*

Proposition 2.8 *Let f_1, f_2 be μ_1, μ_2-conformal mappings, respectively.*

(i) Suppose that f_1, f_2 are defined in the same planar domain and

$$f_2 = h \circ f_1.$$

Then $\mu_1 = \mu_2$ a.e. if and only if h is a conformal mapping from the image of f_1 to the image of f_2.

(ii) Suppose that h is defined in the domain of f_2 and

$$f_2 = f_1 \circ h.$$

If h is conformal, then $\mu_2 = (\mu_1 \circ h)(\overline{h'}/h')$.

(iii) If

$$f_2(z) = \overline{f_1(\overline{z})},$$

then $\mu_2(z) = \overline{\mu_1(\overline{z})}$.

3 Context for Discrete Beltrami Equation

In this section, we describe the geometric and algebraic elements necessary for our discrete version of the Beltrami equation. In particular, we will define the mesh elements appearing in the system to be solved. Then in Sect. 4, we will use this data to write down the specific system of equations.

To discretize the problem, we will use finite triangulations $\mathcal{T}_z$ of the closed unit disk $\overline{\mathbb{D}}$ in the z-plane. We always assume that the support of the triangulation, i.e., the union $|\mathcal{T}_z|$ of the (closed) triangles of $\mathcal{T}_z$, is bounded by a Jordan polygon inscribed in $\overline{\mathbb{D}}$. We are given a proposed Beltrami derivative μ in $\mathbb{D}$, i.e., a measurable function such that $\|\mu\|_\infty = \operatorname{ess\,sup}_{z\in\mathbb{D}} |\mu(z)| < 1$. We want to construct an isomorphic (simplicially equivalent) triangulation $\mathcal{T}_w$ of the unit disk in the w-plane such that the induced piecewise linear mapping (PL-mapping) is approximately μ-conformal on each triangle $\tau \in \mathcal{T}_z$. Note that PL-mappings, which by definition are the unique affine mappings between corresponding triangles of $\mathcal{T}_z$ and $\mathcal{T}_w$, are linear on the common boundary edge of any two adjacent triangles and therefore are necessarily continuous.

While the setting up of the algorithm and its operation can be carried out in the above generality, we will suppose from now on that μ is C^1-smooth since this is the context in which we will be able to prove convergence. We wish to approximate the smooth quasiconformal mapping f satisfying (1), normalized by $f(0) = 0$ and $f(1) = 1$.

3.1 Logarithmic Coordinates

Given μ, in many cases it is not difficult to find a discrete μ-conformal mapping to some triangulation $\mathcal{T}_w$ of a domain whose shape is not predetermined; but the challenge is to make the outer polygon bounding $\mathcal{T}_w$ precisely a circle. This question can be approached many ways, and in general the condition that "the points of the outer polygon of $\mathcal{T}_z$ must be mapped to a circle centered at the origin" translates naturally into some nonlinear conditions, because it involves $|w| = |f(z)|$. In order to evade this boundary condition on $\partial\mathbb{D}$, we can extend $\mu(z)$ by reflection to the exterior of $\mathbb{D}$ (using the chain rule for Beltrami derivatives), likewise extending $\mathcal{T}_z$ by incorporating the vertices $1/\overline{z_{jk}}$, and then we can solve the extended problem on the Riemann sphere. However, the nonlinearity of the inversion $1/\overline{z}$ leads to inaccuracies, since it does not respect affine mappings between triangles. In other words, the inversion in $\{|z| = 1\}$ does not produce a truly symmetric discrete problem. We prefer to avoid this difficulty as follows.

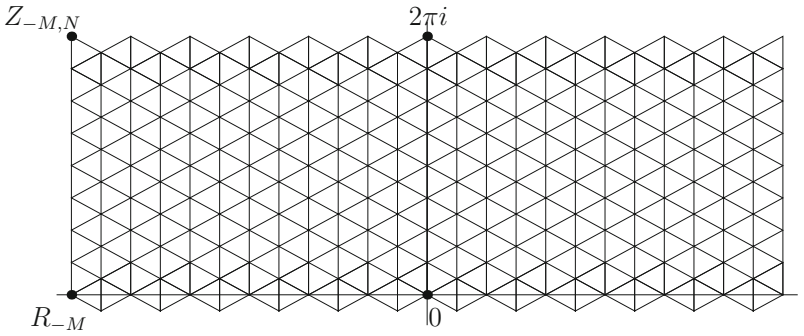

Fig. 1 Basic mesh in *left* Z-plane, together with its reflection in the imaginary axis

We introduce logarithmic coordinates in the form of the variables $Z = \log z$, $W = \log w$ in the left half-plane (cf. [18, part II, section 6.4]). In other words, consider the mapping F from $\{\mathrm{Re}\, Z < 0\}$ to $\{\mathrm{Re}\, W < 0\}$,

$$W = F(Z), \tag{7}$$

defined to be the continuous function in $\{\mathrm{Re}\, Z < 0\}$ determined uniquely by the relation $\exp F(Z) = f(\exp Z)$ and the boundary normalization $F(0) = 0$. Naturally, F is quasiconformal, satisfies the asymptotic condition $\mathrm{Re}\, F(Z) \to -\infty$ as $\mathrm{Re}\, Z \to -\infty$, and inherits the condition $F(z + 2\pi i) = F(z) + 2\pi i$ from the periodicity of exp (this will be essential when we formulate the boundary conditions in 4.1 below, after restricting to a horizontal band). In order to solve for the discrete approximation of the mapping $w = f(z)$ from $\mathbb{D}$ to $\mathbb{D}$, we will solve first for the discretization of F and then simply apply the operation

$$z = \exp(Z), \quad w = \exp(W) \tag{8}$$

to obtain the approximation of the quasiconformal automorphism $z \mapsto w$ of the disk. Of course, we will need to justify that the distortion of triangles produced by the exponential mapping does not affect the accuracy significantly.

3.2 Triangulation

It is convenient to use negative indices for points of the basic domain. We fix the order of the mesh, that is, a pair of positive integers M, N (presumably large). Let

$$R_{-M} < R_{-M+1} < \cdots < R_{-1} < R_0 = 0$$

and define the $(M + 1)N$ vertices

$$Z_{jk} = R_j + \begin{cases} \frac{2\pi k}{N} i, & j \text{ even}, \\ \frac{2\pi (k+1/2)}{N} i, & j \text{ odd}, \end{cases} \tag{9}$$

for $-M \le j \le 0$ and $0 \le k \le N-1$. This is the basic mesh.

If we extend (9) for arbitrary values of k, we obtain a periodic mesh in the vertical direction with $Z_{j,k+N} = Z_{jk} + 2\pi i$. The basic mesh contains MN *rightward pointing triangles* defined as follows:

$$\tau_{jk}^{+} = \begin{cases} (Z_{j-1,k-1},\ Z_{j-1,k},\ Z_{j,k}), & j \text{ even}, \\ (Z_{j-1,k},\ Z_{j-1,k+1},\ Z_{j,k}), & j \text{ odd}, \end{cases} \tag{10}$$

for $-M+1 \le j \le 0$. There are also MN *leftward pointing triangles*

$$\tau_{jk}^{-} = \begin{cases} (Z_{j+1,k-1},\ Z_{j+1,k},\ Z_{j,k}), & j \text{ even}, \\ (Z_{j+1,k},\ Z_{j+1,k+1},\ Z_{j,k}), & j\text{odd}, \end{cases} \tag{11}$$

for $-M \le j \le -1$. Note however, that for even values of j, the triangle τ_{j0}^{+} contains $Z_{j-1,-1}$ and the triangle $\tau_{j,0}^{-}$ contains $Z_{j+1,-1}$; while for odd j, the triangle $\tau_{j,N-1}^{+}$ contains $Z_{j-1,N}$ and the triangle $\tau_{j,N-1}^{-}$ contains $Z_{j+1,N}$. The second index k of each of these points lies outside of the basic range $0 \le k \le N-1$ that most interests us.

We will assume for the rest of this paper that

$$R_j = (\sqrt{3}\,\pi/N)\,j, \tag{12}$$

so the triangles $\tau_{jk}^{\pm}$ will be equilateral. We extend the structure to the right half-plane using the reflection in the imaginary axis

$$\varrho(Z) = -\overline{Z} \tag{13}$$

and setting

$$Z_{jk} = \varrho(Z_{-j,k})$$

for indices $j > 0$. Thus in the extended domain, we have $-M \le j \le M$, with symmetry around the index $j = 0$. The extended triangulation contains $(2M+1)N$ vertices.

Since we are originally given μ in $\mathbb{D}$, we will need the pullback ν of μ as a differential of type $(-1, 1)$ from the disk to the left half-plane (Proposition 2.8); that is,

$$\nu(Z) = \mu(e^Z)\frac{e^{\overline{Z}}}{e^{Z}} = \mu(e^Z)e^{-2i\,\mathrm{Im}\,Z}, \quad \mathrm{Re}\,Z < 0. \tag{14}$$

For $\mathrm{Re}\,Z > 0$, we want $F(Z) = \rho(F(\rho(Z)))$ according to (7). By Proposition 2.8, the Beltrami derivative of F is $\nu(Z) = \overline{\nu(\varrho(Z))}$ for $\mathrm{Re}\,Z > 0$. (Note that in general ν cannot be defined continuously on the full Z-plane, as it does not need to take real values for $\mathrm{Re}\,Z = 0$. However, ν does have right- and left-limits on the imaginary axis that make it a smooth function on either half-plane.). We will write $\nu_{jk}^{\pm}$ for the average value of $\nu(Z)$ on the triangle $\tau_{jk}^{\pm}$. While technically this means the integral of ν divided by the area of the triangle, for numerical work it is convenient and appropriate to take

the average of $\nu(Z)$ over the three vertices as an approximation to this integral, at least when ν is continuous. Let us note that

$$\nu_{jk} = \overline{\nu_{-j,k}}, \quad j > 0. \tag{15}$$

3.3 Boundary Conditions

We will need to describe the behavior of the discrete μ-conformal mapping close to the origin. We write

$$r_j = \exp R_j,$$

so for $j = -M$ the vertical line $\{Z\colon \operatorname{Re} Z = R_{-M}\}$ corresponds to the circle $|z| = r_{-M}$. These latter points may be very small, which is a price we are paying for the use of logarithmic coordinates.

Recall that $f\colon \mathbb{D} \to \mathbb{D}$ denotes the exact (smooth) solution of (1), normalized by $f(0) = 0$, $f(1) = 1$. Near $z = 0$, we know (recall (2), (3)) that f is approximately equal to an affine map $H_{a,0} \circ L_{\mu(0)}$ for some constant $a \in \mathbb{C} \setminus \{0\}$. The image of the small circle is thus close to an ellipse in the w-plane whose eccentricity is determined by $|\mu(0)|$ and whose size and inclination are then determined by the multiplicative factor a. Similarly, the right boundary $\{\operatorname{Re} Z = R_M\}$ corresponds to the inversion of this small ellipse in the circumference $\partial\mathbb{D}$ of $\mathbb{D}$ in the z-plane.

We are thus considering the mapping problem as defined in the annulus $1/r_M \le |z| \le r_M$, which serves as an approximation to the entire plane. The value $|a|$ is related to the conformal module [18] of the image of this annulus under f. Knowledge of the value of a would assist in defining conditions for the mesh points along $\{\operatorname{Re} Z = R_{\pm M}\}$. Let μ_0 denote the average value of $\mu(z)$ inside the small z-circle, and let e_k be the images of the mesh points of this circle under the real-linear mapping L_{μ_0},

$$e_k = L_{\mu_0}(z_{-M,k}) = r_{-M} L_{\mu_0}(e^{2\pi i k/N}), \quad 0 \le k \le N-1.$$

The e_k lie on a small ellipse, and we lift them to the left half-plane as

$$E_k = \log e_k, \tag{16}$$

with $0 \le \operatorname{Im} E_0 < 2\pi$ and $\operatorname{Im} E_{k+1} - \operatorname{Im} E_k < 2\pi$. While it might seem natural to use the values $E_k + \log a$, $\varrho(E_k) + \log a$ in the boundary values for the system of equations to be defined, we will apply a simple modification to sidestep the question of explicitly considering a in 4.2 below, where we give the specific boundary conditions.

4 Discrete Beltrami Equations

Here we define three sets of linear equations to be satisfied by the discrete solution of the Beltrami equation. First we consider the unknowns

$$\{W_{jk}:\ -M \le j \le 0,\ 0 \le k \le N-1\}$$

in the left half-plane and then reflect to the right half-plane.

4.1 Triangle Equations

Following Corollary 2.2, to each rightward pointing triangle τ_{jk}^{+} of (10), we associate one linear equation

$$a_{jk}^{+} W_{jk} + b_{jk}^{+} W_{j-1,k} + c_{jk}^{+} W_{j-1,k+1} = 0, \tag{17}$$

where

$$a_{jk}^{+} = \begin{cases} L_{v_{jk}}(Z_{j-1,k-1} - Z_{j-1,k}), & j \text{ even}, \\ L_{v_{jk}}(Z_{j-1,k} - Z_{j-1,k+1}), & j \text{ odd}, \end{cases}$$
$$b_{jk}^{+} = \begin{cases} L_{v_{jk}}(Z_{j-1,k} - Z_{j,k}), & j \text{ even}, \\ L_{v_{jk}}(Z_{j-1,k+1} - Z_{jk}), & j \text{ odd}, \end{cases}$$
$$c_{jk}^{+} = \begin{cases} L_{v_{jk}}(Z_{j,k} - Z_{j-1,k-1}), & j \text{ even}, \\ L_{v_{jk}}(Z_{jk} - Z_{j-1,k}), & j \text{ odd}, \end{cases}$$

and similarly an equation for each leftward pointing triangle τ_{jk}^{-},

$$a_{jk}^{-} W_{jk} + b_{jk}^{-} W_{j+1,k-1} + c_{jk}^{-} W_{j+1,k} = 0, \tag{18}$$

where

$$a_{jk}^{-} = \begin{cases} L_{v_{jk}}(Z_{j+1,k-1} - Z_{j+1,k}), & j \text{ even}, \\ L_{v_{jk}}(Z_{j+1,k} - Z_{j+1,k+1}), & j \text{ odd}, \end{cases}$$
$$b_{jk}^{-} = \begin{cases} L_{v_{jk}}(Z_{j+1,k} - Z_{j,k}), & j \text{ even}, \\ L_{v_{jk}}(Z_{j+1,k+1} - Z_{j,k}), & j \text{ odd}, \end{cases}$$
$$c_{jk}^{-} = \begin{cases} L_{v_{jk}}(Z_{j,k} - Z_{j+1,k-1}). & j \text{ even}, \\ L_{v_{jk}}(Z_{j,k} - Z_{j+1,k}), & j \text{ odd}. \end{cases}$$

However, while these equations stand as written for values of k giving triangles in the "interior" of our mesh, at the upper and lower parts of the mesh we must take the $2\pi i$-periodicity into account in order to conserve our requirement that $0 \le l \le N-1$ in every appearance of W_{jl}. The exceptions to these equations occur when $k+1 = N+1$ in (17) and when $k-1 = -1$ in (18). When $k = 0$ and j is even, we should use $W_{j\pm1,N-1} - 2\pi i$ in place of $W_{j\pm1,-1}$, while when $k = N-1$ and j is odd, we should write $W_{j\pm1,0} + 2\pi i$ instead of $W_{j\pm1,N}$. Referring to (10) and (11), one sees that the exceptional equations are defined by

$$a^{\pm}_{j0}W_{j0} + b^{\pm}_{j0}W_{j-1,0} + c^{\pm}_{j0}W_{j-1,1} = -2\pi i c^{\pm}_{j0}, \quad j \text{ even},$$
$$a^{\pm}_{j0}W_{j0} + b^{\pm}_{j0}W_{j-1,0} + c^{\pm}_{j0}W_{j-1,1} = 2\pi i b^{\pm}_{j0}, \quad j \text{ odd}. \tag{19}$$

The next step is to "reflect" these equations to the right half-plane via (13). We want F to be symmetric in the imaginary axis: $F = \varrho F \varrho$. Since the Beltrami derivative of this composition is $\nu = \overline{\nu} \circ \varrho$, the prescription (15) indeed reflects ν appropriately to the right half-plane as a discrete Beltrami differential. In other words, consider a triangle $\tau^{\pm}_{jk} = \varrho(\tau^{\pm}_{-j,k})$ in the right half Z-plane ($j \geq 0$). The image $F(\tau^{\pm}_{j,k})$ in the W-plane, defined by W_{jk} and two adjacent vertices, must be the same as $\varrho(F(\tau^{\pm}_{-j,k}))$. It is easily seen that the correspondence $\varrho(\tau^{\pm}_{jk}) \to \varrho(F(\tau^{\pm}_{jk}))$ translates into equations of the same form as (17), (18) with $j \geq 0$ and with the coefficients

$$a^{\pm}_{jk} = \overline{a^{\pm}_{-j,k}}, \; b^{\pm}_{jk} = \overline{b^{\pm}_{-j,k}}, \; c^{\pm}_{jk} = \overline{c^{\pm}_{-j,k}}. \tag{20}$$

So far we have described how the triangles of the extended Z-triangulation provide $4MN$ linear equations: $2MN$ from the left half-plane and another $2MN$ via (20).

4.2 Boundary and Normalization Equations

Next we look at the right and left boundary conditions. As described in 3.3, we have the values E_k, which are the liftings to the left half-plane of a rotated and rescaled version of points along the small ellipse approximating the image of the smallest circle in the mesh $\mathcal{T}_z$.

To avoid the difficulty related to the unknown conformal module of the region between the small ellipse and its inversion, we express a condition that reflects the situation that the image of the circle of radius r_{-M} is an unknown (complex nonzero) multiple of the ellipse $\{e_k\}$. In logarithmic coordinates, the condition is that the image of the curve $\{Z_{-M,k}\}_k$ is a translate of the curve $\{E_k\}_k$ by a complex constant. Similar considerations apply to the reflected curve $\{\varrho(E_k)\}_k$. The boundary equations that express this are the $2(N-1)$ equations

$$W_{-M,k} - W_{-M,k-1} = D_k,$$
$$W_{M,k} - W_{M,k-1} = \overline{D_k}, \tag{21}$$

where $D_k = E_k - E_{k-1}$ and $1 \leq k \leq N-1$. It is important that the magnitude of r_{-M} (which will vary as the mesh is refined) does not influence the value of D_k.

Finally, for normalization of the solution we add one more equation,

$$W_{0,0} = 0, \tag{22}$$

which is self-symmetric. This says that $F(0) = 0$, or equivalently, $f(1) = 1$.

5 Statement and Proof of Main Theorem

The linear system that we will study consists of the triangle, boundary, and normalization equations described in the preceding section, except that for numerical considerations we renormalize each triangle equation by dividing all coefficients by one of $a^{\pm}_{jk}, b^{\pm}_{jk}, c^{\pm}_{jk}$, thus obtaining the proportional values such as

$$\frac{a^{\pm}_{jk}}{c^{\pm}_{jk}},\ \frac{b^{\pm}_{jk}}{c^{\pm}_{jk}},\ 1,$$

and similarly dividing the right-hand sides in (19) by the common factor. As a consequence of Proposition 2.4 (and obvious facts regarding the boundary and normalization equations), the absolute values of all coefficients appearing in the system are bounded above and below by values $(\delta_{\mu_0})^{\pm 2}$ determined by $\|\mu\|_\infty$ alone, independently of the fineness of the mesh. It is irrelevant which of $a^{\pm}_{jk}, b^{\pm}_{jk}, c^{\pm}_{jk}$ is used to normalize the triangle equations; to be definite, we will adopt the following rule: the coefficient corresponding to the rightmost (resp. leftmost) vertex of each rightward- (resp. leftward-) pointing triangle will have coefficient equal to 1.

This linear system contains more equations than variables: there are

$$n_{\mathrm{v}} = (2M+1)N \tag{23}$$

unknowns W_{jk}, $-M \le j \le M$, $0 \le k \le N-1$, and

$$n_{\mathrm{e}} = 4MN + 2(N-1) + 1 \tag{24}$$

equations. Therefore we will use the standard least-squares approximation method [4] to find a solution. To describe the system it is convenient to rename the variables in a single vector $V \in \mathbb{C}^{n_{\mathrm{v}}}$ with

$$V_p = W_{jk}, \tag{25}$$

where $p = p(j,k)$ is given by an arbitrary but fixed bijective correspondence from the set of index pairs $\{(j,k)\colon\ -M \le j \le M,\ 0 \le k \le N-1\}$ to the range $1 \le p \le n_{\mathrm{v}}$. We will write $V = \underline{W}$ or $W = \underline{V}$ to indicate this renaming of the indices.

The equivalent linear system with this normalization now takes the form $A\underline{W} = B$ or

$$AV = B, \tag{26}$$

where $A = (A_{np})$ is a complex $n_{\mathrm{e}} \times n_{\mathrm{v}}$ matrix and $B = (B_n)$ is a complex vector of length n_{e}. When considering the mesh $\{Z_{jk}\}$ as fixed, we will say that (A, B) is the *associated linear system* to the collection of v-values $\{v_{jk}\}$ (recall that the coefficients depend on both v_{jk} and Z_{jk}).

5.1 Statement of Theorem

Our algorithm may be summarized as follows:

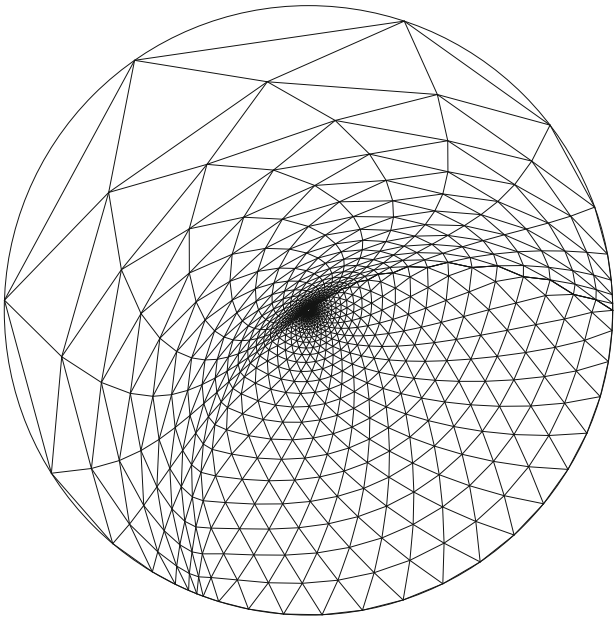

Fig. 2 Different constants in *upper* and *lower* w-half-planes. Note the normalizations $f(0) = 0$, $f(1) - 1$

1. Given a proposed Beltrami derivative μ in $\mathbb{D}$, choose the dimensions M, N for a triangular mesh $\{Z_{jk}\}$ in the Z-plane and calculate the averages v_{jk} of the pullback of $\mu(z)$ to the Z-plane via (14).
2. Calculate the coefficients of the linear system (A, B) associated with $\{v_{jk}\}$ as prescribed by equations (17)–(22).
3. Apply the method of least squares to calculate the approximation V of the solution of the system $AV = B$ and arrange the entries of V to form the mesh $\{W_{jk}\} = \underline{V}$.
4. Calculate $w_{jk} = \exp W_{jk}$ for $-M \le j \le 0$ and $0 \le k \le N - 1$. The desired mapping is the piecewise linear simplicial mapping such that $z_{jk} \mapsto w_{jk}$ where $z_{jk} = \exp Z_{jk}$.

As an illustration, we show in Fig. 2 the w-triangulation for the Beltrami derivative defined by $\mu(z) = 0.5$ when $\operatorname{Im} z > 0$, and $\mu(z) = 0$ when $\operatorname{Im} z \le 0$. This was calculated with $(M, N) = (32, 32)$. Therefore there are many very small triangles that cannot be seen in the picture, in particular those adjacent to the small bounding ellipse. Note how the image triangles from the lower half-plane appear to be equilateral, and there is a clear dividing line between them and the stretched triangles from the upper half-plane. The stretched triangles are not mutually similar, even though μ is constant, since the similarity class of an image triangle depends upon both the value of μ and the slope of the base of the domain triangle. In Fig. 3, we show the logarithmic W-domain. In this picture, the equilateral triangles are in the upper part, with imaginary parts approximately from π to 2π (near the imaginary axis, they occupy a smaller range).

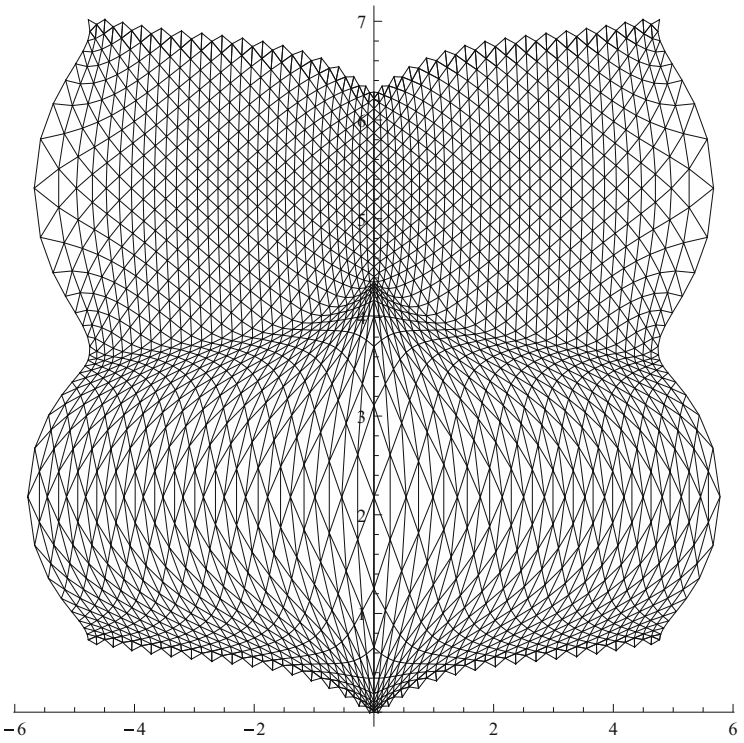

Fig. 3 Different constants in *upper* and *lower* W-half-planes. Note the lifted ellipses at *left* and *right* extremes of the boundary

We now state our main result. Recall that the real parts R_j of the vertices of the logarithmic meshes are given by (12).

Theorem 5.1 *Let μ be a C^1 function in $\mathbb{D}$ with $\|\mu\|_\infty < 1$. Let $M_s, N_s \to \infty$ as $s \to \infty$, where these sequences satisfy*

$$c_1 N_s \log N_s \le M_s \le c_2 N_s \log N_s \tag{27}$$

for constants c_1, c_2, where $c_1 > 1/(\pi\sqrt{3})$. Then:

i. For large s, the points $\{z_{jk}^{(s)}\}$ and the points $\{w_{jk}^{(s)}\}$ produced by the algorithm form the vertex sets of isomorphic triangulations $\mathcal{T}_z^{(s)}$ and $\mathcal{T}_w^{(s)}$ of the unit disk $\mathbb{D}$. Further, any fixed compact set $K \subset \text{int } \mathbb{D}$ is contained in the supports of $\mathcal{T}_z^{(s)}$ and of $\mathcal{T}_w^{(s)}$ for sufficiently large s.

ii. Let $f^{(s)}$ denote the piecewise-linear mapping of $\mathcal{T}_z^{(s)}$ to $\mathcal{T}_w^{(s)}$ that sends $z_{jk}^{(s)}$ to $w_{jk}^{(s)}$ as given by Corollary 2.3. Then the mappings $f^{(s)}$ converge to the solution f of the Beltrami equation (1), normalized by $f(0) = 0$, $f(1) = 1$, as $s \to \infty$, uniformly on compact subsets of $\mathbb{D}$.

5.2 Lemmas

In preparation for the proof of Theorem 5.1, we recall that the statement "$AV = B$" in step 3 of the algorithm translates roughly into the statement that "the PL-mapping $Z \mapsto W$ is $\{\nu_{jk}\}$-conformal". However, the algorithm only produces the least-squares approximation for (A, B), which we will call V'; i.e., the L_2-norm $\|R'\|_2$ of the residual vector

$$R' = AV' - B \tag{28}$$

is the smallest possible.

In Lemmas 5.2 to 5.5, (A, B) is the associated linear system for some fixed collection $\{\nu_{jk}\}$ satisfying $|\nu_{jk}| < 1$, with mesh dimensions M and N.

Since there are many more equations than variables involved, it is not surprising that the system is overdetermined:

Lemma 5.2 *If $X \in \mathbb{C}^{n_v}$ and $AX = 0$, then $X = 0$.*

Proof We examine the role of different rows of A in $AX = 0$. Recall that we write $\underline{X}_{jk}$ for $X_{p(j,k)}$, cf. (25). First note that there appear equations (21) for the "lifted ellipse," with zero on the right-hand side in place of D_k and $\overline{D_k}$. These equations say that $\underline{X}_{-M,k+1} - \underline{X}_{-M,k} = 0$; i.e., all of the $\underline{X}_{-M,k}$ are now of the same value, say c. The equations (17), (19) for the rightward-pointing triangles with $j = -M + 1$ give us

$$a^+_{-M+1,k}\underline{X}_{-M+1,k} + b^+_{-M+1,k}\underline{X}_{-M,k} + c^+_{-M+1,k}\underline{X}_{-M,k'} = 0$$

for suitable k', and using what we have just proved for $j = -M$ and the facts that $a^+_{-M+1,k} \neq 0$ (recalling the remark after Proposition 2.1) and $a^+_{-M+1,k} + b^+_{-M+1,k} + c^+_{-M+1,k} = 0$, we deduce that $\underline{X}_{-M+1,k} = c$ for all k. Continuing this way, we have $\underline{X}_{-j,k} = c$ for all k and $-M \leq j \leq 0$. The normalization equation $\underline{X}_{0,0} = 0$ says that $c = 0$, and then the symmetry gives $\underline{X}_{jk} = 0$ for all j, k. Thus $X = 0$. □

For the next lemma, we consider a hexagon formed of six triangles within the Z-mesh and label the vertices $Z_0, \ldots, Z_6$ as in Fig. 4. (Thus "Z_n" refers to some Z_{jk}, avoiding complications of indices.) Associate with the triangles some constant Beltrami values $\nu_1, \ldots, \nu_6$.

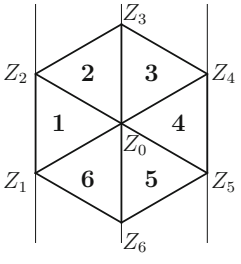

Fig. 4 Hexagonal arrangement within basic mesh

Since the rightmost and leftmost vertices of triangles 1,…,6 are Z_0, Z_2, Z_4, Z_0, Z_5, and Z_1, respectively, the normalized triangle equations take the form

$$\begin{aligned}
V_0 - c_1 V_1 + (c_1 - 1) V_2 &= 0,\\
V_2 - c_2 V_3 + (c_2 - 1) V_0 &= 0,\\
V_4 - c_3 V_0 + (c_3 - 1) V_3 &= 0,\\
V_0 - c_4 V_4 + (c_4 - 1) V_5 &= 0,\\
V_5 - c_5 V_6 + (c_5 - 1) V_0 &= 0,\\
V_1 - c_6 V_0 + (c_6 - 1) V_6 &= 0,
\end{aligned}$$

where V_n is the value corresponding to the point Z_n of the mesh and c_n is easily expressed in terms of ν_n. This is the same as

$$\begin{aligned}
V_0 &= c_1 V_1 + (1 - c_1) V_2,\\
(1 - c_2) V_0 &= V_2 - c_2 V_3,\\
c_3 V_0 &= -(1 - c_3) V_3 + V_4,\\
V_0 &= c_4 V_4 + (1 - c_4) V_5\\
(1 - c_5) V_0 &= V_5 - c_5 V_6,\\
c_6 V_0 &= -(1 - c_6) V_6 + V_1.
\end{aligned} \tag{29}$$

Recall that the least-squares solution V' of a system $AV = B$ is given explicitly by $V' = (A^H A)^{-1} A^H B$, where A^H is the conjugate transpose of A. In particular, a system of the simple form $\{\alpha_n V_0 = \beta_n\}$, with a single unknown, has the least-squares solution

$$V_0' = \frac{\sum \overline{\alpha_n} \beta_n}{\sum |\alpha_n|^2}, \tag{30}$$

into which we may substitute the explicit values of (29).

By continuity of ν, as the mesh is refined, we will have approximately $\nu_1 = \cdots = \nu_6$. For this particular case, the solution is given by

$$\begin{aligned}
V_0' = {} & \frac{1}{|1-c|^2 + |c|^2 + 1} \left(c \frac{V_1 + V_4}{2} + (1 - c) \frac{V_2 + V_5}{2} \right)\\
& + \frac{|c|^2}{|1-c|^2 + |c|^2 + 1} \left(\frac{1}{c} \frac{V_1 + V_4}{2} + \left(1 - \frac{1}{c} \right) \frac{V_3 + V_6}{2} \right)\\
& + \frac{|1-c|^2}{|1-c|^2 + |c|^2 + 1} \left(\frac{1}{1-c} \frac{V_2 + V_5}{2} + \frac{-c}{1-c} \frac{V_3 + V_6}{2} \right).
\end{aligned}$$

This is a convex combination of three values, each of which is a (complex) convex combination of averages of values associated to opposite vertices of the hexagon.

In the following result, we do not suppose that all six Beltrami coefficients are necessarily equal.

Lemma 5.3 *Let V' be the least-squares solution of the full linear system $AV = B$. Let $V'_1, \ldots, V'_6$ be the selected values of V' corresponding to the vertices $Z_1, \ldots, Z_6$ of the hexagon. Let $v_1, \ldots, v_6$ be the values of the discrete Beltrami coefficient used to define the system in the triangles of the hexagon. Then the value V'_0 in V' corresponding to the center Z_0 of the hexagon is exactly equal to the least-squares solution (30) of the hexagon subsystem (29) in which V_n is replaced by V'_n, $1 \le n \le 6$.*

Proof The full system has a residual R' defined by (28) that has minimal possible L_2-norm. Recalling (29), we may separate the norm calculation into two sums,

$$\|R'\|_2^2 = \sum_{n=1}^{6} |\alpha_n V'_0 - \beta_n|^2 + \sum_{n=7}^{n_e} |R'_n|^2,$$

where β_n ($1 \le n \le 6$) are expressions involving $V'_1, \ldots, V'_6$. The only appearances of V'_0 in this calculation of $\|R'\|_2^2$ are in the six terms of the first sum on the right-hand side, since the only triangles containing Z_0 as a vertex lie in the hexagon under consideration. Therefore the second sum is not affected by the value of V'_0, so the minimum residual for the full system is obtained only when the first sum is the minimum possible for the given values of $V'_1, \ldots, V'_6$. □

Remark 5.4 Lemma 5.3 has a far-reaching generalization. Suppose that we are given sets of indices $\Gamma, \Omega \subseteq \{(j,k): \ -M \le j \le M, \ 0 \le k \le N-1\}$, where the vertices Z_{jk} for $(j,k) \in \Gamma$ trace a simple closed polygon properly enclosing those vertices with indices in Ω. Consider the subsystem of $A\underline{W'} = B$ consisting of all those equations that contain variables W'_{jk} such that $(j,k) \in \Sigma$. Then these equations only contain W'_{jk} such that $(j,k) \in \Sigma \cup \Omega$. Write these equations with the variables in Ω on the left-hand side and the variables in Σ on the right. Assign to the Σ-variables the values of the least-squares solution for the full $n_e \times n_v$ system $A\underline{W'} = B$. Then the least-squares solution for the Ω-values of the reduced system also coincide with the values for the full system. Note that Lemma 5.3 corresponds to the particular case in which Σ corresponds to $\{V'_1, \ldots, V'_6\}$ and Ω corresponds to $\{V'_0\}$. The proof is the same except for complexity of notation. One may replace Ω by the exterior instead of the interior of Γ, and in fact one can relax somewhat the condition that Γ traces a simple closed polygon.

Lemma 5.5 *(i) For any $W = \{W_{jk}\}$ ($-M \le j \le M$, $0 \le k \le N-1$), the following symmetry relation holds:*

$$A\underline{\overleftrightarrow{W}} = A\underline{\varrho(W)},$$

where $\overleftrightarrow{W}_{jk} = W_{-j,k}$, $\varrho(W) = \{\varrho(W_{jk})\}$, and ϱ is defined by (13). (ii) Let V' be the solution of the linear system (26) produced by the method of least squares. Then the entries of $W' = \underline{V'}$ satisfy the symmetry $W'_{-j,k} = \rho(W'_{jk})$. In particular, the central values W'_{0k} are purely imaginary.

Proof (i) The relation $A\overleftrightarrow{W} = A\varrho(W)$ follows immediately from the previous symmetry relations such as (20). (ii) By Lemma 5.2, A has full column rank, so the vector that minimizes the L_2-norm of the residual $\|AV - B\|_2$ is unique [4]. Therefore $\overleftrightarrow{W'} = \varrho(W')$. □

In the following, recall the distance between similarity classes of triangles discussed in 2.2. Background material on triangulations of manifolds may be found in [22].

Lemma 5.6 *Let $\mathcal{T}_z$ be a triangulation of (a polygon inscribed in) the disk $\mathbb{D}$. Let $f : |\mathcal{T}_z| \to \overline{\mathbb{D}}$ be a local homeomorphism. Suppose that f sends each triangle of $\mathcal{T}_z$ in a 1-to-1 manner onto a Euclidean triangle, preserving orientation. Suppose further that f sends the boundary points of $\mathcal{T}_z$ (by hypothesis on $\partial\mathbb{D}$) to $\partial\mathbb{D}$. Then the images under f of the vertices of $\mathcal{T}_z$ form a triangulation $\mathcal{T}_w$ of $\mathbb{D}$, and f is a homeomorphism from $|T_z|$ onto $|\mathcal{T}_w|$.*

Proof Note that $f(|\mathcal{T}_z|)$ is bounded. Write $D = \operatorname{int}\mathcal{T}_z$. We claim that $f(D) \subseteq \mathbb{D}$. Otherwise the boundary of $f(D)$ would contain a point p exterior to $\mathbb{D}$ and there would be a sequence $\{z_n\}$ in D such that $f(z_n) \to p$. Now z_n must accumulate in the closure of D, and in fact to a boundary point $z_0 \in \partial D$ since f is a local homeomorphism. Thus z_0 is on an edge of a triangle joining two points of $\partial\mathbb{D}$, and p is on the corresponding edge of the image triangle, which by the hypothesis on boundary points must lie in $\overline{\mathbb{D}}$, a contradiction that proves the claim.

From this it follows easily that f satisfies the path-lifting property, and thus is a covering map of simply connected regions, so it is a homeomorphism. Therefore the image of $\mathcal{T}_z$ is a triangulation contained in $\mathbb{D}$ and isomorphic to $\mathcal{T}_z$. □

5.3 Proof of Main Theorem

We divide the proof of Theorem 5.1 into several steps.

(1.) First we note that it suffices to prove the theorem under the assumption that μ *admits a C^1-smooth extension to a neighborhood of* $\overline{\mathbb{D}}$. Indeed, for $0 < r < 1$, the approximations $\mu_r(z) = \mu(rz)$ satisfy this condition, converge to μ pointwise as $r \to 1$, and are uniformly bounded below $\|\mu\|_\infty$, so by Proposition 2.7, the associated normalized quasiconformal mappings converge uniformly to the solution $f = f_\mu$ of $(\partial f/\partial z)/(\partial f/\partial z) = \mu$. Then the conclusions of the theorem are easily transferred to f from these approximating mappings. We henceforth assume that μ extends smoothly up to the boundary.

Next we verify that f sends sufficiently small equilateral triangles to triangles of the same orientation (note that this need not hold for large triangles in $\mathbb{D}$). Near an interior point $z_0 \in \mathbb{D}$, this is a consequence of the differentiability of f, which is approximated near z_0 by its Jacobian $J_f|_{z_0}$, a nonsingular linear mapping (cf. the measure of discrepancy from being equilateral described in Sect. 2.2 above, and further discussion of $J_f|_{z_0}$ in steps (3.) and (4.) below). Suppose now instead that $z_0 \in \partial\mathbb{D}$. The extension of μ to $\mathbb{C}$ by reflection along $\partial\mathbb{D}$ may have distinct limits when approaching z_0 from the interior and exterior, but we will now see that at any rate f enjoys a certain type of "regularity" at z_0.

Let $\{|z| < 1\}$ correspond to $\{\mathrm{Im}\,\zeta > 0\}$ under a Möbius transformation taking z_0 to $\zeta_0 \in \mathbb{R}$, and use this transformation to pull back μ to a Beltrami differential λ defined in $\{\mathrm{Im}\,\zeta > 0\}$. Then extend λ by reflection via $\lambda(\overline{\zeta}) = \overline{\lambda(\zeta)}$. We may as well assume $\zeta_0 = 0$. Consider the limiting values a, $\overline{a}$ of $\lambda(\zeta)$ as $\zeta \to 0$ within $\{\mathrm{Im}\,\zeta > 0\}$ or $\{\mathrm{Im}\,\zeta < 0\}$, respectively. Let $\widetilde{f}$ be a global λ-conformal mapping leaving $\mathbb{R}$ invariant; thus $\widetilde{f}(\zeta)$ differs from $f(z)$ by a Möbius transformation. We wish to compare $\widetilde{f}$ with the quasiconformal mapping g where $g(\zeta) = L_a(\zeta)$ for $\mathrm{Im}\,\zeta > 0$ and $g(\zeta) = L_{\overline{a}}(\zeta)$ for $\{\mathrm{Im}\,\zeta < 0\}$ (recall (2)). Thus we consider the composition $h = \widetilde{f} \circ g^{-1}$, which coincides with $\widetilde{f}$ along $\mathbb{R}$.

Note that $(L_a)^{-1} = L_b$, where $b = a(1 + \overline{a})/(1 + a)$. From this and the chain rule, we find that the Beltrami differential κ of the mapping $h = \widetilde{f} \circ L_b$ in the upper half-plane is given by

$$\kappa = \frac{b + (\lambda \circ L_b)\frac{1+b}{1+\overline{b}}}{1 + b(\lambda \circ L_b)\frac{\overline{b}(1+b)}{b(1+\overline{b})}} = \frac{1+\overline{a}}{1+a}\,\frac{-a + (\lambda \circ L_b)}{1 - \overline{a}(\lambda \circ L_b)}$$

and a similar formula (replacing a, b with their conjugates) in the lower half-plane. Since $\lambda(L_b(0))$ and $\lambda(L_{\overline{b}}(0))$ are the limiting values a and $\overline{a}$, these two chain rule formulas show that κ is continuous at $\zeta = 0$ and $\kappa(0) = 0$. Further, κ inherits from λ the property that its restrictions to the upper and lower half-planes have smooth extensions across the boundary (which do not necessarily coincide with the values of κ in the opposite half-plane.) Thus $|\kappa(\zeta)| = O(|\zeta|)$ near $\zeta = 0$, so the integral

$$\iint \frac{|\kappa(\zeta)|}{|\zeta^2|}\,|d\zeta|^2$$

is finite in a neighborhood of 0. By [18, Section 7.1, p. 233], we have that h is conformal at the origin in the sense that $h(\zeta)/\zeta$ has a nonzero finite complex limit. (This same result of [18] can be used to justify the claims we have made previously regarding the smoothness of f.)

Returning to $\mathbb{D}$, we conclude that the similarity classes of triangles near z_0 are not altered too much by f (i.e., bounded by an amount corresponding to the value a), so in particular, the image triangles do not degenerate or have their orientation reversed. Finally, by covering $\mathbb{D}$ by finitely many appropriate neighborhoods, we have our assertion that small triangles are sent by f to triangles of the same orientation.

Now by Lemma 5.6, the solution $f = f_\mu$ of $(\partial f/\partial z)/(\partial f/\partial z) = \mu$ sends sufficiently fine equilateral triangulations to triangulations. Statement (i) of the theorem will follow when we prove that the algorithm produces a sufficiently good approximation to f.

Before proceeding, we note that the pullback ν of μ given by (14) is C^1 smooth in the left half-plane (up to the boundary) and is periodic of period $2\pi i$, while the solution $F = F_\nu$ of $(\partial F/\partial Z)/(\partial F/\partial Z) = \nu$ is C^2 there, with the limiting conditions $F(\infty) = -\infty$, $F(0) = 0$. Note again that in general the extension of F by reflection in the imaginary axis is not C^1 on the axis itself.

(2.) We now begin to derive growth conditions on the elements of the associated linear system. The condition (27) implies that

$$r_{-M} < \frac{1}{N}, \tag{31}$$

so further,

$$|z_{-M,k} - z_{-M,k-1}| < \frac{2\pi}{N} r_{-M} = O\left(\frac{1}{N^2}\right), \tag{32}$$

where $M = M_s$, $N = N_s$, $s \to \infty$.

We restrict our attention to the mesh $\mathcal{T}_{MN}$. We must relate the approximation W' to the values

$$\underline{V} = W = F(\mathcal{T}_{MN})$$

of the true ν-conformal mapping F at the vertices of the basic mesh.

By Lemma 5.6, W is a triangulation when the values M, N are large enough. Fix such M, N, and let $\nu_{MN} = \{(\nu_{MN})^{\pm}_{jk}\}$ denote the collection of average values of the function ν on the triangles of $\mathcal{T}_{MN}$. Recall that the associated linear system $(A, B) = (A_{MN}, B_{MN})$ used in the algorithm is defined in terms of the values of ν_{MN}.

Let F^*_{MN} denote the PL-mapping on the support of $\mathcal{T}_{MN}$ defined by the condition $\mathcal{T}_{MN} \to W$. Thus by construction, F^*_{MN} coincides with F on the vertices of $\mathcal{T}_{MN}$ (both map to W), but the Beltrami derivative of F^*_{MN} is constant on each triangle. We will write ν^*_{MN} for this collection of constants.

Let $(A^*, B^*) = (A^*_{MN}, B^*_{MN})$ be the linear system associated with the discrete Beltrami coefficient ν^*_{MN} for fixed values of M, N. Recalling (28), we will compare the following:

$$A\underline{W'} - B = R', \tag{33}$$

$$A^*\underline{W} - B^* = \varepsilon. \tag{34}$$

(3.) The vector $\varepsilon = \varepsilon_{MN}$ defined in (34) is described as follows. The entries of ε corresponding to the triangle equations are 0, because F^*_{MN} is ν^*_{MN}-conformal and takes $\mathcal{T}_{MN}$ to W. Therefore, the only nonzero values in ε are in the positions corresponding to the boundary equations. By (21), the values in $A^*\underline{W}$ are $F(Z_{-M,k}) - F(Z_{-M,k-1})$, while the values in B^* are $E_k - E_{k-1}$, so in the corresponding positions, ε contains the value

$$(F(Z_{-M,k}) - E_k) - (F(Z_{-M,k-1}) - E_{k-1}).$$

To estimate this, we recall that f is of class C^2 and use the approximation

$$f(z) = (J_f|_0)(z) + O(|z|^2)$$

at the origin, where the Jacobian is given by $J_f|_0 = H_{a,0} \circ L_{\mu(0)}$ for some complex $a \neq 0$. Thus by (31), $f(z_{-M,k}) = ae_k + O(N^{-2})$. From (32), we see that

$$\frac{f(z_{-M,k})e_{k-1}}{f(z_{-M,k-1})e_k} = \frac{(ae_k + O(N^{-2}))e_{k-1}}{(ae_{k-1} + O(N^{-2}))e_k} = \frac{e_k e_{k-1} + O(N^{-2})}{e_k e_{k-1} + O(N^{-2})} = 1 + O(N^{-2}).$$

Taking logarithms, we conclude that the nonzero entries of ε shrink at least as fast as $O(N^{-2})$. We will write $O(\varphi_1(N)/\!/\varphi_2(N)/\!/\varphi_3(N))$ to indicate the respective growth bounds $O(\varphi_i(N))$ on the entries of vectors in $\mathbb{C}^{n_v}$ corresponding to the normalization/boundary/triangle equations. Thus we have

$$\varepsilon = O(0/\!/N^{-2}/\!/0). \tag{35}$$

(4.) In practice, one applies the algorithm by using average values

$$\nu_{MN}(T) = \frac{\nu(Z_1) + \nu(Z_2) + \nu(Z_3)}{3} \tag{36}$$

for $T = (Z_1, Z_2, Z_3) \in \mathcal{T}_{MN}$. It is a simple exercise to verify that this differs from the value $(\int_T \nu\, dx\, dy)/\text{area}(T)$ by an amount that tends to zero as $O((\text{diam } T^2)) = O(N^{-2})$. Since ν is differentiable, we have $\nu(Z_i) = \nu(Z_0) + (J_\nu|_{Z_0})(Z_i - Z_0) + O(N^{-2})$, $i = 1, 2, 3$, where we take $Z_0 = (Z_1 + Z_2 + Z_3)/3$. It is immediate from (36) that

$$\nu_{MN}(T) = \nu(Z_0) + O(N^{-2})$$

as the triangulation is refined and Z_0 always refers to the center of the triangle T.

On the other hand, consider

$$\begin{aligned} W_i = F(Z_i) &= F^*(Z_i) = W_0 + (J_f|_{Z_0})(Z_i - Z_0) + O(N^{-2}) \\ &= W_0 + H_{a,b} \circ L_{\nu(Z_0)}(Z_i - Z_0) + O(N^{-2}) \end{aligned} \tag{37}$$

(where the constants a, b depend on Z_0), and recall that $\nu^*_{MN}(T)$ is given by Corollary 2.3; i.e.,

$$\begin{aligned} \nu^*_{MN}(T) = &- \frac{(Z_2 - Z_1)(W_3 - W_1) - (Z_3 - Z_1)(W_2 - W_1)}{(\overline{Z_2} - \overline{Z_1})(W_3 - W_1) - (\overline{Z_3} - \overline{Z_1})(W_2 - W_1)} \\ &= \nu(Z_0) + O(N^{-1}), \end{aligned}$$

as is seen by applying (2)–(3) in (37) and cancelling. We conclude that

$$|\nu^*_{MN} - \nu_{MN}| = O(N^{-1}). \tag{38}$$

(5.) Observe that entries of (A, B) and (A^*, B^*) in any given position come from identical explicit formulas, using data ν^*_{MN} and ν_{MN}, respectively. By Corollary 2.2,

entries in A, A^* resulting from normalized triangle equations are of the form $\pm L_\nu(Z_i - Z_j)/L_\nu(Z_i - Z_k)$, $\pm L_{\nu^*}(Z_i - Z_j)/L_{\nu^*}(Z_i - Z_k)$, respectively, where a given triangle is referred to by (Z_1, Z_2, Z_3) as in (36), and ν, ν^* refer here to the constant values assigned to that particular triangle. The difference is

$$\frac{L_\nu(Z_i - Z_j)}{L_\nu(Z_i - Z_k)} - \frac{L_{\nu^*}(Z_i - Z_j)}{L_{\nu^*}(Z_i - Z_k)} = \frac{2\,\mathrm{Im}\,(Z_i - Z_j)(\overline{Z_i} - \overline{Z_k})}{L_\nu(Z_j - Z_k)L_{\nu^*}(Z_j - Z_k)}(\nu^* - \nu).$$

Since $|\nu|$, $|\nu^*|$ are bounded away from 1 as $N \to \infty$, by Corollary 2.5 the coefficient of $\nu^* - \nu$ in the above expression is bounded, having both numerator and denominator of precise order N^{-2}. By (38), this difference corresponding to triangle equations is at most $O(N^{-1})$. The entries of A, A^* resulting from boundary or normalization equations do not depend on ν, ν^* and cancel out upon subtraction. We thus have shown the first of the two following estimates:

$$\text{columns of } (A^* - A) = O(0/\!/0/\!/N^{-1}), \quad B^* - B = O(0/\!/N^{-2}/\!/0), \tag{39}$$

and we now verify the second estimate in detail. From (16), the entries of B, B^* in the positions of the boundary equations are

$$E_k - E_{k-1},\ E_k^* - E_{k-1}^*,$$

determined respectively using the values given by ν, ν^*. Thus we use power series expansions to estimate

$$\begin{aligned} B^* - B &= \log \frac{1 + \mu^* e^{-4\pi i k/N}}{1 + \mu^* e^{-4\pi i (k-1)/N}} - \log \frac{1 + \mu e^{-4\pi i k/N}}{1 + \mu e^{-4\pi i (k-1)/N}} \\ &= \log(1 \\ &\quad + (\mu^* e^{-4\pi i k/N} + \mu e^{-4\pi i (k-1)/N} - \mu^* e^{-4\pi i (k-1)/N} - \mu e^{-4\pi i k/N}) \\ &\quad + \cdots) \\ &= \log(1 + (\mu^* - \mu)(e^{-4\pi i k/N} - e^{-4\pi i (k-1)/N}) + \cdots \\ &= \log(1 + O(N^{-2})) \;=\; O(N^{-2}) \end{aligned}$$

as we claimed.

Now we can estimate $(A - A^*)\underline{W}$. By construction, each row of A or A^* contains at most three nonzero entries, inasmuch as only three variables appear in equations (17), (18), etc. The entries of $(A - A^*)\underline{W}$ are then of the form $\sum_p (A_{np} - A^*_{np})V_p$, where for each n, at most three of the n_{v} summands are nonzero. If we represent the coefficients of the normalized triangle equations by A_1, A_2, A_3, A_1^*, A_2^*, A_3^* with $A_1 + A_2 + A_3 = 0$, $A_1^* + A_2^* + A_3^* = 0$, we find

$$\begin{aligned} ((A^* - A)V)_n &= (A_1V_1 + A_2V_2 + A_2V_3) - (A_1^*V_1 + A_2^*V_2 + A_2^*V_3) \\ &= (A_1 - A_1^*)(V_1 - V_3) + (A_2 - A_2^*)(V_2 - V_3). \end{aligned}$$

Here $V_1 - V_3$, $V_2 - V_3$ are differences of adjacent W_{jk} vertices, with $W_{jk} = F(Z_{jk})$. The preimage differences $Z_1 - Z_3$, $Z_2 - Z_3$ are of order N^{-1}, and since F is differentiable, we have $V_1 - V_3$, $V_2 - V_3 = O(N^{-1})$ also. By (39), we conclude that $\max_n((A^* - A)\underline{W})_n = O(N^{-2})$, so

$$(A^* - A)\underline{W} = O(0/\!/0/\!/N^{-2}). \tag{40}$$

(6.) From the definition (34) and the estimates (35), (39), (40), we have that

$$A\underline{W} - B = (A - A^*)\underline{W} + \varepsilon + (B^* - B) = O(0/\!/N^{-2}/\!/N^{-2}).$$

Since vectors in $\mathbb{C}^{n_v}$ have 1 normalization term, $O(N)$ boundary terms, and $O(MN) = O(N^2 \log N)$ triangle terms, the L_2-norm satisfies the bound

$$\begin{aligned} \|A\underline{W} - B\|_2 &= O(\,(1 \cdot 0^2 + N \cdot (N^{-2})^2 + (N^2 \log N) \cdot (N^{-2})^2))^{1/2}\,) \\ &= O(N^{-1}(\log N)^{1/2}). \end{aligned}$$

By minimality of $\|A\underline{W'} - B\|_2 = \|R'\|_2$ (recall (28)) and by (35), we have

$$\|R'\|_2 \le \|A\underline{W} - B\|_2,$$

so

$$\|R'\|_2 = O(N^{-1}(\log N)^{1/2}). \tag{41}$$

According to (33), this may be be interpreted loosely as saying that $\underline{W'}$ satisfies the linear system (A, B) to within certain precision. We will bound the cardinality

$$d = \#\{n\colon\ |R'_n| \ge (N \log N)^{-1}\}.$$

Clearly $dN^{-2}(\log N)^{-2} \le \sum_{n=1}^{n_e} |R'_n|^2 = \|R'\|_2^2 = O(N^{-2} \log N)$, so

$$d = O((\log N)^3).$$

Since the total number of contributions to the residual is $n_e \sim MN \sim N^2 \log N$, this shows that $|R'_n| < (N \log N)^{-1}$ except possibly for a collection of indices n that grows arbitrarily sparse in $\{1 \le n \le n_e\}$. Actually, due to the tendency of the least-squares solution to spread the error as efficiently as possible (recall Remark 5.4), one would expect the value of the entries $|R_n|$ to be in fact of the order $O(N^{-2})$, since

$$n_e(N^{-2})^2 \sim (N^2 \log N)N^{-4} = N^{-2} \log N,$$

which is the order of the growth bound (41) we showed for $\|R'\|_2^2$ above.

Consider a triangle equation

$$a_1 W_1 + a_2 W_2 + a_3 W_3 = \epsilon,$$

where $\epsilon = O((N \log N)^{-1})$. If ϵ were zero, then Corollary 4 would give that the triangle (W_1, W_2, W_3) has the similarity class dictated by the corresponding value of ν_{jk} as the image of the equilateral triangle (Z_1, Z_2, Z_3). This similarity class can also be described as having two edges with the complex ratio $-a_2/a_1$. As it is, assuming that $|W_2 - W_3|$ is of the same order N^{-1} as is $|Z_2 - Z_3|$, we can estimate

$$\frac{W_1 - W_3}{W_2 - W_3} = -\frac{a_2}{a_1} + \frac{\epsilon}{W_2 - W_3} = -\frac{a_2}{a_1} + O((\log N)^{-1});$$

i.e., the density of the triangles in the mesh whose similarity classes fail to approach that of a ν-conformal mapping must tend to zero as the mesh is refined. In particular, these triangles share the orientation of Z_1, Z_2, Z_3.

The above argument requires that $N|W_2 - W_3|$ is bounded below. Noting that in the j-th column of the mesh,

$$|W_{j,N-1} - W_{j,0}| \le \sum_{k=1}^{N-1} |W_{j,k} - W_{j,k-1}|,$$

we see that if $|W_{j,k} - W_{j,k-1}| = o(N^{-1})$, then the height $|W_{j,N-1} - W_{j,0}|$ of the column of triangles tends to zero. However, an exceptional triangle equation (19) gives a relation that implies that $W_{j,N-1} \pm 2\pi i$, $W_{j-1,0}$, and $W_{j-1,1}$ form a small positively oriented triangle, which makes $W_{j,N-1}$, on the contrary, at a distance of approximately 2π from $W_{j,0}$. Thus the W-triangles cannot be too small.

The approximately-satisfied boundary equations (21) tell us that the left and right boundaries of the mesh are sent approximately to the lifted ellipses. In this regard, note that the continuity of $\mu(z)$ at $z = 0$ in $\mathbb{D}$ implies that the values of $\mu(e^Z)$ on the right-hand side of (14) are approximately equal to the constant $\mu(0)$ when $Z = Z_{jk}$ with j close to $-M$. Therefore the portion of the linear system involving vertices near the left boundary $j = -M$ consists of equations that describe the discretization of the function $\log L_{\mu(0)}(e^Z)$ (cf. the leftmost portion of Fig. 3).

Thus the boundary of the image of $\mathcal{T}_{MN}$ forms a Jordan polygon for large enough N. Most of the triangles in this image are positively oriented, with possible exceptions numbering at most d/n_e. However, applying again Remark 5.4, we can surround groups of such exceptional vertices by Jordan trajectories Ω that are mapped properly, and since there certainly exists a way to fill in the interior of Ω by triangles that are approximately ν- (or ν^*-) conformal, the least-squares solution also fulfills this condition.

Finally, we observe that $W'_{00} = 0$ for the following reason. If one and the same constant is added to every element of W', none of the equations in the linear system will be affected except for the normalization equation. Therefore the least-squares residual is minimized when the normalization is satisfied exactly, as claimed.

We have proved that the points $W' = \underline{V'}$ produced by the algorithm differ by an arbitrarily small amount from the image vertices under the true ν-conformal mapping $W = F(Z)$.

(7.) Finally, we apply the exponential mapping via (7) and (8) to obtain the sequence of PL-mappings $f^{(s)}\colon z \mapsto w$ of subdomains that exhaust the unit disk $\mathbb{D}$, produced by the algorithm for the meshes determined by (M_s, N_s). These are indeed mappings by Lemma 5.6.

Let $\epsilon > 0$, and consider the annulus $\mathbb{D}_\epsilon = \{\epsilon < |z| < 1\}$. The image $f(\mathbb{D}_\epsilon)$ is approximately the part of $\mathbb{D}$ outside of a small ellipse. By construction, the correspondence $F\colon Z \mapsto W$ extends by $2\pi i$-periodicity to a mapping of the left half-plane $\{\operatorname{Re} Z \le 0\}$ to $\{\operatorname{Re} W \le 0\}$, as do all the approximants $F^{(s)}$. The extended quasiconformal mapping F is uniformly continuous on the band $\{-1/\epsilon \le \operatorname{Re} Z \le 0\}$, so the diameters of the W-triangles in the images of triangles contained in this band tend uniformly to zero as $s \to \infty$. Consider such a triangle (W_1, W_2, W_3) and its image (w_1, w_2, w_3), where $w_i = \exp W_i$. We compare the angle at W_1, which is $\arg(W_3 - W_1)/(W_2 - W_1)$, with the angle

$$\arg \frac{w_3 - w_1}{w_2 - w_1} = \arg\left(\frac{e^{(W_1+W_3)/2}}{e^{(W_1+W_2)/2}} \cdot \frac{\sin(W_3 - W_1)}{\sin(W_2 - W_1)} \right)$$

at w_1. The first factor on the right-hand side is $e^{(W_3-W_2)/2} \to 1$ since $|W_3 - W_2| \to 0$. The second factor tends to $(W_3 - W_1)/(W_2 - W_1)$, again uniformly in the band. As a consequence, the exponential mapping sends W-triangles to approximately similar w-triangles (thus in particular respecting the orientation), and the procedure provides a triangulation of $f^{(s)}(\mathbb{D}_\epsilon)$ for which the induced PL-mapping $f^{(s)}|_{\mathbb{D}_\epsilon}$ is approximately μ-conformal. The limit as $s \to \infty$ is μ-conformal, fixes $z = 1$, and hence coincides with the mapping of doubly connected domains $f|_{\mathbb{D}_\epsilon}\colon \mathbb{D}_\epsilon \to f(\mathbb{D}_\epsilon)$. Since ϵ is arbitrary, we conclude that $f^{(s)} \to f$. This completes the proof. □

6 Numerical Results

All of the calculations have been done with machine precision in *Mathematica* on a standard laptop computer of approximately 1GH. We have not found any examples where more precision will make a difference. The *Mathematica* routine `LeastSquares` handles sparse matrices [4,26], a data structure that registers only the nonzero entries appearing in a matrix or vector.

In the first several examples, we compare the results produced by our algorithm with an exact formula for the quasiconformal mapping under consideration.

Example 1 A simple test case is for constant $\mu(z) = c$. There is an explicit formula [25] for the conformal mapping to $\mathbb{D}$ from an ellipse with semimajor and semiminor axes of lengths a, b $(a^2 - b^2 = 1)$ and foci at ± 1,

$$w = \sqrt{k}\, \mathrm{sn}\,(\frac{2K}{\pi} \sin^{-1} u; k^2), \tag{42}$$

where the Jacobi elliptic function modulus k is related to the complete elliptic integral K and the Jacobi theta functions by the formulas

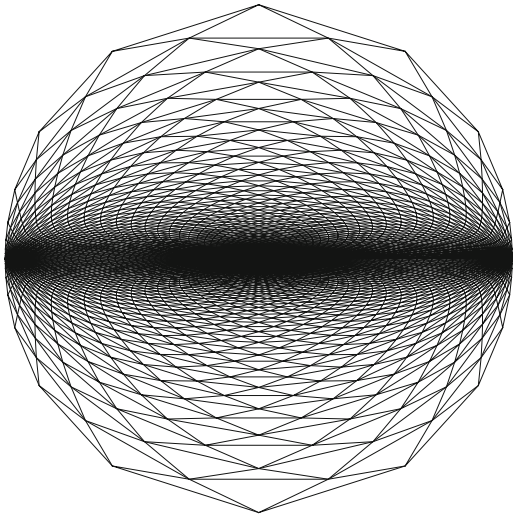

Fig. 5 Image for constant Beltrami derivative $\mu = 0.5$ and $(M, N) = (52, 64)$. Observe the "crowding phenomenon" at the boundary

$$q = (a+b)^{-4} = e^{-\pi K(1-m)/K(m)},$$
$$k = \sqrt{m} = \left(\frac{\theta_2}{\theta_3}\right)^2,$$

with notation from [27]. Note that the image of the circle $|z| = 1$ under the mapping L_μ is an ellipse with semiaxes 1, $(1-|\mu|)/(1+|\mu|)$ slanted in the directions $(1/2)\arg\mu$, $(1/2)(\arg\mu + \pi)$, respectively, modulo π. This ellipse is sent by the conformal linear mapping $H_{1/(2\sqrt{\mu}),0}$ to the ellipse with semiaxes a, b. Then via (42) this is transformed conformally to the unit disk.

It is well known that a conformal mapping from an ellipse to a disk tends to "crowd" boundary points near the images of the endpoints of the major axis. The crowding, or maximum ratio of separation of N points sent to the Nth roots of unity, increases exponentially as a function of the aspect ratio a/b [10, section 2.6]. In contrast, the affine mapping L_μ that we combined with this conformal mapping produces little crowding. The combined effect is a great deal of crowding near $w = 1$, as can be perceived in Fig. 5.

The algorithm of Theorem 5.1 was applied for the constant Beltrami derivatives $\mu = 0.1,\ 0.3,\ 0.5,\ 0.7$, and meshes defined by $N = 16, 32, 48, 64, 72, 84$, with M equal to the least multiple of 4 no less than $N \log N/(\pi\sqrt{3})$, in view of (27). In the last case, there are 24,359 equations in 14,196 variables. It took about 1.5 s to calculate the part of the matrix in the left half-plane and about 10 s to solve the full set of equations. Table 1 presents the maximum error over all w_{jk} when these points are compared to the images of z_{jk} under the exact quasiconformal mapping described in the preceding paragraph. As is to be expected, the error increases when the Beltrami derivative increases, but decreases when the mesh is refined. It was found that for $\mu = 0.7$ and a rather coarse mesh such as $(M, N) = (36, 48)$, the image of $\mathcal{T}_{MN}$ is not a triangulation, inasmuch as a few of the w-triangles near ± 1 are improperly

Table 1 The maximum of the absolute errors between the solutions and the real values of some constant Beltrami derivative and $M \approx N \log N/(\pi\sqrt{3})$

(M, N)	(12,16)	(24,32)	(36,48)	(52,64)	(60,72)	(72,84)
$\mu = 0.1$	0.012	0.0031	0.0014	0.0008	0.0006	0.0004
$\mu = 0.3$	0.0274	0.007	0.0031	0.0018	0.0014	0.001
$\mu = 0.5$	0.0615	0.0205	0.0109	0.0065	0.0051	0.0038
$\mu = 0.7$	0.2439	0.1201	0.0856	0.0627	0.053	0.0412

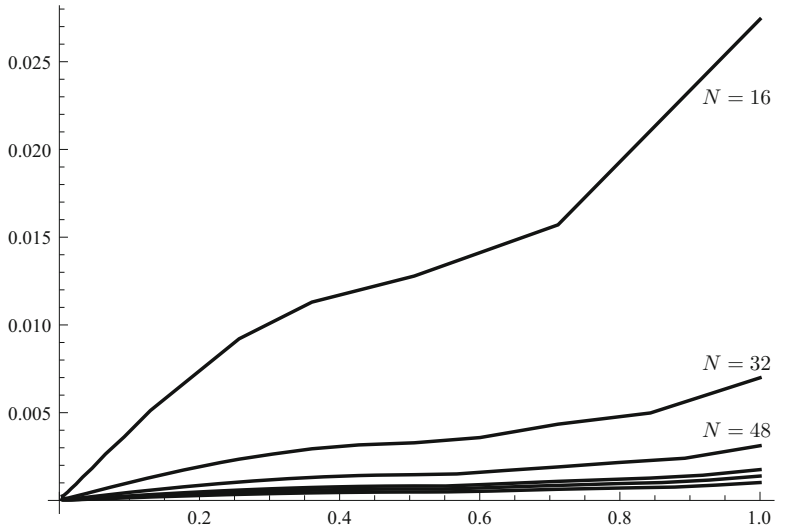

Fig. 6 Numerical errors of algorithm for different values of (M, N) with $\mu = 0.3$. The *horizontal axis* indicates the distance $r_j = |z_{jk}|$ of the z-points from the origin; the *vertical axis* gives the maximum discrepancy (over k) of the calculated value of w_{jk} from the true value

oriented. In spite of this fact, the values obtained for the conformal mapping are not very far off.

We give a further analysis of the variation of the error as a function of the radius for the particular value $\mu = 0.3$. Figure 6 shows the maximum error over k in the calculated value of w_{jk} for each fixed j. It is seen that the error remains approximately constant for $r < 0.7$ and then increases rather sharply for $0.7 < r < 1$. Thus the maximum values in Table 1 are much higher than the average errors. As noted above, the maximum error, which occurs on the boundary, decreases as a function of N.

Example 2 Radial quasiconformal mapping. Let $\varphi\colon [0, 1] \to [0, 1]$ be an increasing diffeomorphism of the unit interval. Then the radially symmetric function

$$f(z) = \varphi(|z|)e^{i \arg z} = \varphi(|z|)\frac{z}{|z|} \tag{43}$$

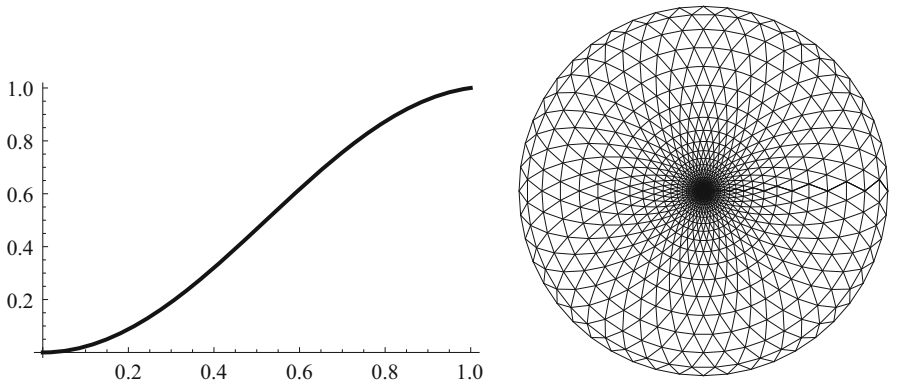

Fig. 7 Radial function φ of example 2 (*left*), together with the induced rotationally symmetric image domain

Table 2 Maximum absolute error for radially symmetric function with μ mapping defined by (44)

(M,N)	(12,16)	(24,32)	(36,48)	(52,64)	(60,72)	(72,84)
Error	0.0398	0.0135	0.0058	0.0034	0.0027	0.0020

has Beltrami derivative equal to

$$\mu(z) = \frac{|z|\varphi'(z)/\varphi(z) - 1}{|z|\varphi'(z)/\varphi(z) + 1}\frac{z}{\overline{z}} \tag{44}$$

when $z \neq 0$. As an illustration, we will take

$$\varphi(r) = (1 - \cos 3r)/(1 - \cos 3)$$

as in Fig. 7. The resulting Beltrami derivative satisfies $\|\mu\|_\infty = 0.65$ approximately.

The domain points z_{jk} on the real axis were selected, and the values of w_{jk} produced by the algorithm were compared with the true values $\varphi(|z_{jk}|)$. The results are given in Table 2. It was also observed that as in the previous example, the errors increase as the radius increases.

Example 3 Sectorial quasiconformal mapping. In a similar spirit, we consider an increasing diffeomorphism $\psi : [0, 2\pi] \to [0, 2\pi]$. We write $\widetilde{\psi}(e^{i\theta}) = e^{i\psi(\theta)}$. Then the sectorially symmetric function

$$f(z) = |z|\,\widetilde{\psi}\left(\frac{z}{|z|}\right) \tag{45}$$

has Beltrami derivative equal to

$$\mu(z) = \frac{1 - \psi'(\theta)}{1 + \psi'(\theta)}\frac{z}{\overline{z}} \tag{46}$$

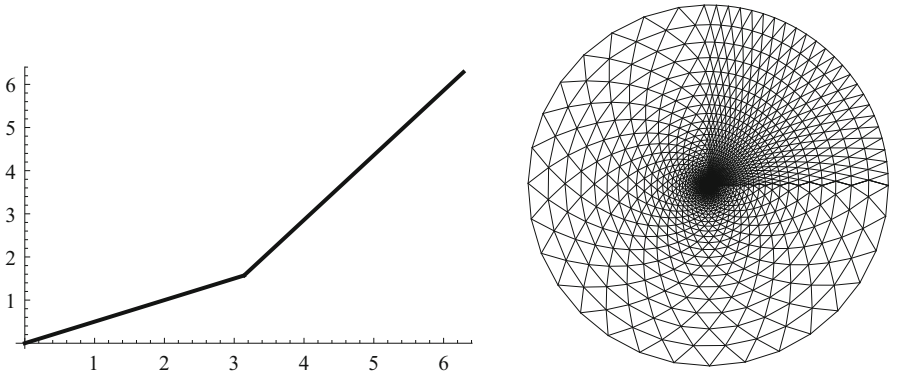

Fig. 8 Angular function ψ of example 3 (*left*), together with image domain under sectorial mapping (45)

Table 3 Maximum absolute error $|\psi(\theta) - f(e^{i\theta})|$ for sectorial mapping with μ defined by (46)

(M,N)	(12,16)	(24,32)	(36,48)	(52,64)	(60,72)	(72,84)
Error	0.0712	0.0362	0.0251	0.0193	0.0173	0.0150

when $z \neq 0$. As an example, we will take

$$\psi(\theta) = \begin{cases} \frac{\theta}{2}, & 0 \leq \theta \leq \pi, \\ \frac{\pi}{2} + \frac{3(\theta-\pi)}{2}, & \pi \leq \theta \leq 2\pi, \end{cases}$$

as in Fig. 8. In this example, μ does not satisfy the hypotheses of Theorem 5.1 because it is not continuous. The arguments of the final boundary values on the unit circle were compared with the true values $\psi(\theta)$; see Table 3.

Example 4 Exterior mappings. In Daripa [7], quasiconformal mappings from $\mathbb{D}$ to the exterior of an ellipse (the origin being sent to ∞) are calculated with the following two sample Beltrami derivatives:

$$\mu_1(z) = |z|^2 e^{0.65(iz^5 - 2.0)},$$
$$\mu_2(z) = \frac{1}{2}|z|^2 \sin(5\mathrm{Re}\, z).$$

These exterior mapping results can be related to those of our algorithm by use of the rational function

$$h(z) = \frac{(1+\alpha) - (1-\alpha)z^2}{2\alpha z},$$

which transforms $\mathbb{D}$ conformally to the exterior of an ellipse with aspect ratio α. Composition of h following the quasiconformal self-mapping of D provides a mapping to the exterior of the ellipse with the same Beltrami derivative.

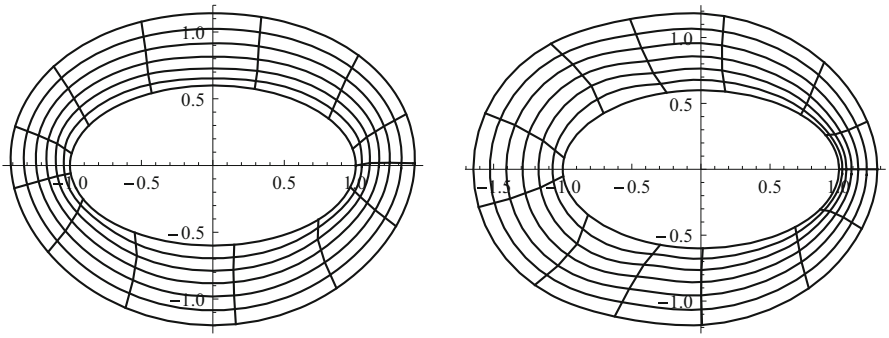

Fig. 9 Self-mappings of unit disk with Beltrami derivatives μ_1 (*left*), μ_2 (*right*), followed by conformal mapping to exterior of ellipse as in [7]

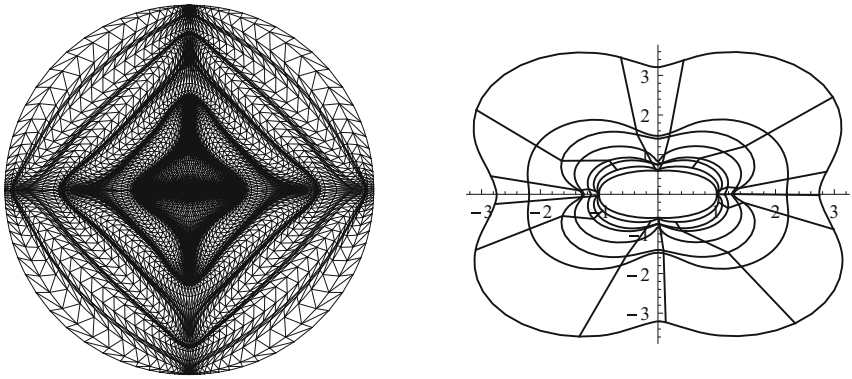

Fig. 10 Quasiconformal mappings to disk (*left*) and exterior of ellipse (*right*) determined by (47)

In the examples in [7], $\alpha = 0.6$ is specified (however, the inner ellipses in [7] appear to have aspect ratios of approximately 0.47; axes are not drawn.) We have made adjustment for the fact that Daripa uses M radii equally spaced in $[0, 1]$, in contrast to the exponential spacing we have been using. Our results are depicted in Fig. 9 with $(M, N) = (64, 64)$. These images appear fairly similar those shown in [7].

Computation times are reported in [7] for $N = 64$ as approximately 8.5 s of CPU on a MIPS computer described as "approximately 15 times slower than the CRAY-YMP at Texas A & M University" of that time. Our laptop CPU times, using *Mathematica*, were approximately 15 s for the first example and 45 s for the other.

It is apparent from the examples in [7] that Beltrami derivatives with a great deal of oscillation were used in order to create an interesting problem. Figure 10 shows our results for the mapping of the disk to the exterior of the same ellipse, with Beltrami derivative

$$\mu(z) = 0.9 \sin |20z| \tag{47}$$

and $(M, N) = (128, 128)$.

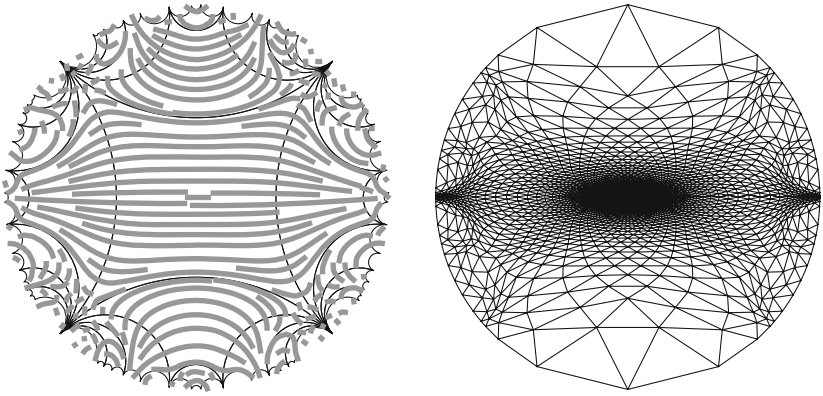

Fig. 11 (*left*) *Horizontal* trajectories of quadratic differential Φ (48); (*right*) image triangulation arising from induced Teichmüller differential (50), which effectively produces a stretching along these trajectories

(5) *Quasiconformal deformation of Fuchsian groups.* In this example, μ is associated with a quadratic differential for a Fuchsian group (see [13,17] for definitions). The two linear-fractional transformations

$$z \mapsto \frac{z + \sqrt{2}/2}{(\sqrt{2}/2)z + 1}, \quad z \mapsto \frac{z + i\sqrt{2}/2}{-i(\sqrt{2}/2)z + 1}$$

generate a free group Γ of self-mappings acting freely on $\mathbb{D}$. This group has a standard fundamental domain with fourfold symmetry about the origin as shown in Fig. 11, and the quotient Riemann surface $\mathbb{D}/\Gamma$ is homeomorphic to a torus with a single puncture. We create a holomorphic function in $\mathbb{D}$ via the Poincaré series

$$\Theta(z) = \sum_{\gamma \in G} (\gamma'(z))^2, \tag{48}$$

which is known to converge and to satisfy the invariance relation

$$\Theta(\gamma(z))\gamma'(z)^2 = \Theta(z) \tag{49}$$

for every γ in Γ. Then for $0 \le |c| < 1$, the function

$$\mu(z) = c\frac{\overline{\Theta(z)}}{\Theta(z)} \tag{50}$$

is a Beltrami differential for the group Γ; that is, $\mu(\gamma(z))\overline{\gamma'(z)}/\gamma(z) = \mu(z)$ for every γ in Γ. This implies that the normalized μ-conformal self-mapping $f_c\colon \mathbb{D} \to \mathbb{D}$ satisfies $f_c(\gamma(z)) = \gamma_c(f_c(z))$, where $\gamma \mapsto \gamma_c$ is an isomorphism from Γ to another Fuchsian group Γ_c also acting on $\mathbb{D}$. A large part of Teichmüller theory is devoted to understanding the nature of deformed groups such as Γ_c and their dependence on μ.

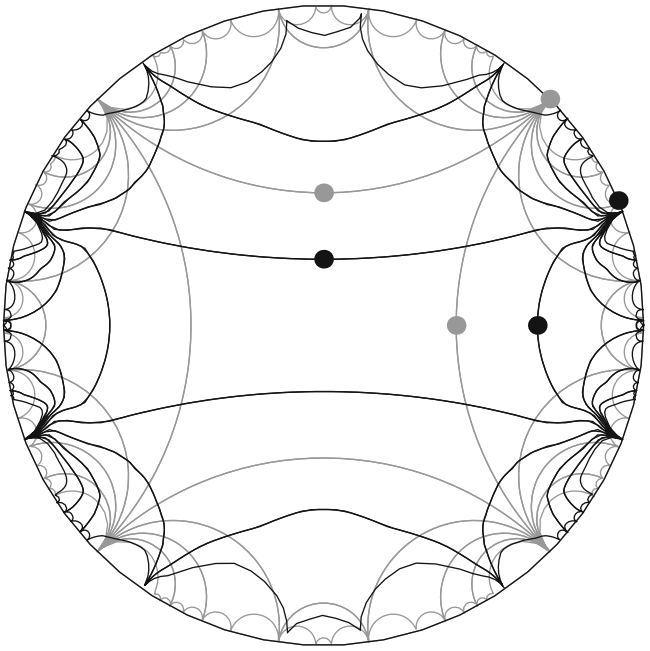

Fig. 12 Self-mapping of unit disk, with Beltrami derivative defined via a Poincaré series. Computations were made with $(M, N) = (64, 64)$. The standard fundamental domain (*lighter contour*) is symmetric under rotation by $\pi/2$; its image under the quasiconformal mapping (*black contour*) is superimposed

Figure 11 shows the trajectory structure of the quadratic differential Φ, that is, the solutions of $\Phi(z)dz^2 > 0$, together with a w-triangulation obtained from the μ-conformal mapping for $c = 0.5$. Figure 11 shows the w-triangulation for $(M, N) = (64, 64)$. Figure 12 is a superposition of the z- and w-domains, with part of the tessellation of $\mathbb{D}$ by group translates of the fundamental domain of Γ and also the tessellation by their images, which are fundamental domains for Γ_μ. The images were calculated by taking each point defining each curve of the original tessellation, identifying the particular z-triangle in which it lies, and then applying the PL-mapping to the corresponding w-triangle of Fig. 11. Some inaccuracies, particularly near the boundary, are clearly visible inasmuch as the image curves must be hyperbolic geodesics. One probable source of error is in the calculation of $\Theta(z)$. To evaluate (48), we truncated the series to words of up to length 6 in the generators of Γ and/or inverses, and used (49) to apply (48) directly only for z inside the fundamental domain containing the origin; then (50) was applied for points outside the fundamental domain.

An independent verification of this mapping is made using the results of [5] on conformal mapping of symmetric quadrilaterals with circular sides. In the present context, where the vertex angles of the fundamental domains are all equal to zero, such quadrilaterals depend (up to conformal equivalence) on two real parameters, which may be prescribed in several ways, some relating to the geometry of the circular quadrilateral (such as the midpoints p_1, p_2 of the right and upper edges as marked in Fig. 12), others relating to parameters in the conformal mapping. In particular, there is

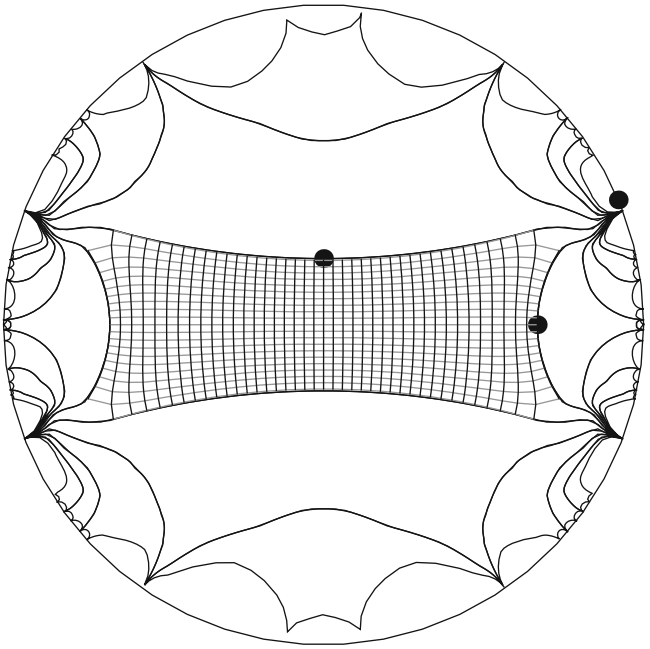

Fig. 13 Comparison of the image of the basic fundamental domain via quasiconformal mapping and conformal mapping techniques. The trajectories inside the fundamental domain were calculated as the images under the conformal mapping of *vertical* and *horizontal* segments in the period *rectangle* of the Weierstrass $\wp$-function

a conformal mapping h from a Euclidean rectangle with vertices at $\pm\omega_1 \pm \omega_2$ ($\omega_1 > 0$, $\omega_2/i > 0$) to the fundamental domain quadrilateral, whose Schwarzian derivative $\mathcal{S}_h$ [1] is equal to the following elliptic function:

$$\mathcal{S}_h(\zeta) = \frac{1}{2}\wp(\zeta + \omega_1 + \omega_2) - 2\sigma, \tag{51}$$

where the essential parameter is the purely imaginary ratio $\tau = \omega_2/\omega_1$, which determines the second parameter $\sigma = \sigma(\tau) \in \mathbb{R}$ due to the fact that the circular edges must be orthogonal to the circle passing through the four image vertices $h(\pm\omega_1 \pm \omega_2)$. Here ω_1, ω_2 are basic half-periods of the Weierstrass $\wp$-function, normalized in a specific way that we will not describe here. Methods are given in [5] for calculating the relationships among these parameters. We have applied them to the observed values for $p_1 = f_c(\sqrt{2} - 1)$ and $p_2 = f_c(i(\sqrt{2} - 1))$ obtained from our algorithm for the Beltrami equation, together with the fact that $\tau = (1-c)/(1+c)$, to obtain the value of σ numerically. Then the Schwarzian differential equation (51) was solved, first along the real and imaginary axes, and from there along vertical and horizontal lines throughout the rectangle with vertices $\pm\omega_1 \pm \omega_2$. Since this was done with a normalization of $h'(0) = 1$, a further scaling was necessary to adjust the size to match the value of p_1. It is seen (Fig. 13) that the midpoint p_2 and the curvatures of the edges agree quite well (Table 4). In general, if one is interested in deforming Fuchsian or Kleinian groups by

Table 4 Relative error of midpoint p_2 of the upper edge of the deformed fundamental domain compared to result of conformal mapping from the rectangle. Calculations made with $M = N$

c	τ	$N = 16$	$N = 32$	$N = 48$	$N = 64$
0.1	0.818	0.022	0.006	0.003	0.002
0.3	0.538	0.089	0.027	0.011	0.008
0.5	0.333	0.283	0.110	0.052	0.031

this method, a reasonable strategy would be to replicate the information obtained in such a fundamental domain via the group action of Γ_c.

7 Discussion and Conclusions

It is stated in Daripa [7] that prior to that article there were no constructive methods published for solving the Beltrami equation in the disk numerically. Convergence proofs appeared later in [11] together with a modified scheme. There are other methods that also include convergence proofs (we have mentioned [14,28]) but without giving a detailed analysis of the rate of convergence. Therefore we discuss here some aspects of [7,11] in relation to our algorithm. As we mentioned in the Introduction, that approach is based on evaluation of singular integrals. The original problem is presented in the context of finding a μ-conformal mapping to a prescribed star-shaped domain and is in some ways reminiscent of the classical method of Theodorsen [15] for conformal mappings.

Daripa's main algorithm requires evaluation of the $\partial/\partial\overline{z}$ derivatives that appear in the singular integrals. A variant is also proposed that does not require these derivatives; however, this is not applied in the numerical examples provided. The operation count of one iteration of Daripa's method is $O(MN \log N)$. This should be multiplied by the average number of iterations required, which depends on how refined the mesh is and how much accuracy is desired. In the examples that we have taken from [7], $\|\mu\|_\infty$ is approximately 0.5, but it should be noted that $|\mu(z)|$ is in fact bounded by 0.12 for $|z| < 0.5$ and by 0.05 for $|z| < 0.3$. In fact, an important limitation stated in [7] is that the Beltrami derivative μ must be Hölder continuous. Further, it is recommended that μ vanish at least as fast as $|z|^3$ at the origin for the method to work properly. In [11], it is similarly recognized that computation time increases as $\|\mu\|_\infty$ increases. Our algorithm, in contrast, is not subject to any such requirement on μ. Our computation times are considerably longer than those reported in [11], but this may be due in large part to use of a symbolic interpreter rather than a compiled program.

We also mention the method presented in [21] for determining a Teichmüller mapping to an arbitrary domain. It begins by choosing an "optimal" Beltrami derivative and then solving the corresponding boundary Beltrami equation. A system of linear equations is determined to discretize this equation, which must be solved together with a collection of nonlinear boundary constraints. This is solved by an iterative method (conjugate gradient).

Our algorithm involves no evaluation of singular integrals and no iteration of solutions. As described in Sect. 5, we use a purely linear system (A, B). For a mesh of dimensions M, N, the matrices A, B are of orders $n_e \times n_v$, $n_e \times 1$, respectively, where

n_e and n_v are given by (23) and (24). Although the total number of elements contained in A is $O(M^2N^2)$, by construction A is a sparse matrix. As we noted during the proof of Theorem 5.1, the number of nonzero elements of any row of A is no greater than 3. Further, the number of nonzero elements of any column of A is no greater than 7 (note that each variable W_{jk} in (17), (18) corresponds to a vertex of at most six triangles, cf. Fig. 1; the only vertex appearing in seven equations is $W_{0,0}$, cf. (22)). Hence the number of nonzero elements in A is no greater than $O(MN)$.

Since the linear system $AV = B$ is highly overdetermined and in general there is no exact solution, we have used the least squares approximation. There are many numerical methods available for the least squares problem; a comprehensive reference is [4]. For simplicity, we discuss the method of "normal equations," that is, the solution of $A^H AV = A^H B$. It is easily seen that by construction, the columns of A are linearly independent, so that $A^H A$ is positive definite, and each row or column of $A^H A$ contains at most 7 nonzero entries. These entries are not consecutive, but the index correspondence in (25) may be taken so that the row bandwidth of $A^H A$ is $2M$. When one applies Gaussian reduction to (A, B), the nth of the n_v rows will only need to reduce at most $2M$ of the succeeding rows, and will require no more than $2M$ floating-point multiplications for each one. Thus the total operation count is of the order of $O(n_v(2M)^2) = O(M^3N)$. Once $A^H A$ has been thus reduced to echelon form, the computational cost of back substitution is seen to be no more than $O(M^2N)$. These computations do not require a significant amount of storage other than the original data. In summary, when one doubles the mesh dimensions M, N, the memory requirement is at most multiplied by 4 (which is the same as the increase in the mesh itself) and the computation time by 16. Our numerical experiments indicate that the more sophisticated least-squares algorithms found in packaged software appear to reduce these exponents slightly.

The symmetry of the linear system in the left and right half-planes implies that $W_{0,k} - \overline{W_{0,k}} = 0$. One could take this as a boundary condition for a system on the left half-plane alone. However, that would convert the system into one involving the real variables $\operatorname{Re} W_{jk}$, $\operatorname{Im} W_{jk}$ instead of the original complex variables, and thus would not in reality reduce the order of the matrices under consideration, nor would it change the fact that the system is overdetermined. Since it involves real instead of complex arithmetic, it could possibly be used to optimize the computation somewhat. One can introduce many other variants, such as using values of R_j in (9) that are not equally spaced. For example, r_j could be equally spaced, which might give a more natural way to cut up the unit disk. However, our use of equilateral triangles has greatly facilitated the estimates in the proof of the main theorem. We mention that we have tried many other strategies, such as working outward along concentric triangulated annuli and minimizing various quantities representing the error in the quasiconformality dilatation (mostly nonlinear operations), but so far have not found a method as effective as the one presented here.

Naturally, the problem on the entire z-plane could be formulated in terms of a variety of other types of meshes, for example, a large square partitioned in any of several possible ways. If such a mesh were to be used, for example, to solve the Beltrami equation in $\mathbb{D}$ by extending μ as zero in $\mathbb{C} \setminus \mathbb{D}$, one could take advantage of the simple asymptotic behavior at ∞ in order to set the boundary conditions there.

Afterwards, a numerical conformal mapping method could be applied on the image of $\mathbb{D}$ to obtain a self mapping of $\mathbb{D}$. (As we alluded to in 3.1, this is an example of a nonlinear approach.) While this would no doubt be possible and would be worth investigating, we note that it would not offer the advantage of automatically leaving $\partial\mathbb{D}$ invariant (an essential characteristic of the problem we have treated), and as one is often interested in the behavior of the solution precisely on the boundary, it may require a denser mesh there. Further, the conformal mapping method would need to deal with the crowding phenomenon on $\partial\mathbb{D}$ (recall Fig. 5) and may fail to produce a result if the quasiconformal step is not sufficiently accurate. In our method, even when an algorithm is used for least squares that involves successive approximations for solving the linear system numerically, it would probably not be greatly affected, say, by a few points lying in the incorrect order along the boundary during an intermediate step. Many conformal mapping methods are somewhat delicate in this regard. Additionally, we note that our method requires no work at all related to constructing an appropriate mesh adapted to a given problem.

It may be noted that our algorithm can also be used for solving the Beltrami equation on the entire z-plane (normalized by fixing 0, 1, and ∞) instead of the disk. One simply eliminates the step of extending the Beltrami coefficient from the disk to its exterior by reflection. We have not yet investigated this question numerically.

Finally, we assert that it seems probable that our algorithm will converge to the μ-conformal mapping even when μ is only piecewise smooth, and perhaps in even greater generality. Many numerical examples suggest this, some of which we have given above. The estimates in the proof of Theorem 5.1 concerning L_2 norms would not be greatly affected if only a small proportion of the terms in the sums failed to tend to zero as fast as required. We hope to look into these questions in future work.

We believe that this algorithm for solving the Beltrami equation is conceptually much simpler than other methods that have been presented, and is easy to implement.

Acknowledgments The authors are grateful to T. Sugawa for many critical and useful comments in the preparation of this work, as well as to the referees who uncovered some significant errors in the first version and made numerous useful suggestions (in particular the use of [18, Section 7.1]). The first author is also grateful to D. Marshall for pointing out several fundamental errors in the approach proposed in [23]. This paper forms part of the second author's Ph.D. thesis.

References

1. Ahlfors, L.: Lectures on Quasiconformal Mappings, 2nd edition, University Lecture Series 38. American Mathematical Society, Providence, RI (2006)
2. Angenent, S., Haker, S., Tannenbaum, A., Kikinis, R.: Laplace–Beltrami operator and brain surface flattening. IEEE Trans. Med. Imaging **18**, 700–711 (1999)
3. Astala, K., Mueller, J.L., Perämäki, A., Päivärinta, L., Siltanen, S.: Direct electrical impedance tomography for nonsmooth conductivities. Inverse Probl. Imaging **5**, 531–549 (2011)
4. Björck, Å.: Numerical Methods for Least Squares Problems. SIAM (1996). ISBN 978-0-89871-360-2
5. Brown, P., Porter, R.M.: Conformal mapping of circular quadrilaterals and Weierstrass elliptic functions. Comput. Methods Funct. Theory **11**, 463–486 (2011)
6. Daripa, P., Mashat, D.: An efficient and novel numerical method for quasiconformal domains. Numer. Algorithms **18**, 159–175 (1998)
7. Daripa, P.: A fast algorithm to solve the Beltrami equation with applications to quasiconformal mappings. J. Comput. Phys. **106**, 355–365 (1993)

8. Daripa, P.: On applications of a complex variable method in compressible flows. J. Comput. Phys. **88**, 337–361 (1990)
9. Daripa, P.: A fast algorithm to solve nonhomogeneous Cauchy–Riemann equations in the complex plane. SIAM J. Sci. Stat. Comput. **13**, 1418–1432 (1992)
10. Driscoll, T.A., Trefethen, L.N.: Schwarz–Christoffel Mapping. Cambridge Monographs on Applied and Computational Mathematics, vol. 8. Cambridge University Press, Cambridge (2002)
11. Gaidashev, D., Khmelev, D.: On numerical algorithms for the solution of a Beltrami equation. SIAM J. Numer. Anal. **46**(5), 2238–2253 (2008)
12. Gu, X.D., Zeng, W., Luo, F., Yau, Sh-T: Numerical computation of surface conformal mappings. Comput. Methods Funct. Theory **11**, 747–787 (2011)
13. Harvey, W.J. ed.: Discrete Groups and Automorphic Functions. In: Proceedings of an Instructional Conference held in Cambridge, July 28–August 15, 1975. Academic Press (1977)
14. He, Zh-X: Solving Beltrami equations by circle packing. Trans. A.M.S. **322**, 657–670 (1990)
15. Henrici, P.: Applied and Computational Complex Analysis, vol. 3. Wiley, New York (1986)
16. Kamenetskiĭ, D.S., Tsynkov, S.V.: On the construction of images of simply connected domains realized by solutions of a system of Beltrami equations (Russian). Akad. Nauk SSSR Inst. Prikl. Mat. Preprint no. 155 (1990)
17. Lehto, O.: Univalent Functions and Teichmüller Spaces. Springer, New York (1995)
18. Lehto, O., Virtanen, K.I.: Quasiconformal Mappings in the Plane, 2nd Edition, Die Grundlehren der Mathematischen Wissenschaften, vol. 126. Springer, New York (1973)
19. Lévy, B., Petitjean, S., Ray, N., Maillot, J.: Least Squares Conformal Maps for Automatic Texture Atlas Generation, ACM Transactions on Graphics (TOG). In: Proceedings of ACM SIGGRAPH 2002, **21**, 362–371 (2002)
20. Lui, L.M., Lam, K.C., Wong, T.W., Gu, X.: Texture map and video compression using Beltrami representation. SIAM J. Imaging Sci. **6**, 1880–1902 (2013)
21. Lui, L.M., Lam, K.C., Yau, S.-T., Gu, X.: Teichmüller mapping (T-map) and its applications to landmark matching registration. SIAM J. Imaging Sci. **7**(1), 391–426 (2014)
22. Munkres, J.R.: Elementary Differential Topology. Lectures Given at Massachusetts Institute of Technology, Fall, 1961. Revised edition. Annals of Mathematics Studies, vol. 54, Princeton University Press, Princeton, N.J
23. Porter, R.M.: Numerical Solution of the Beltrami Equation. arXiv:0802.1195 [math.CV]
24. Samsoniya, Z.V.: Construction of certain quasiconformal mappings (Russian). Trudy Vychisl. Tsentra Akad. Nauk Gruzin. SSR **23**, 76–89 (1983)
25. Szegö, G.: Conformal mapping of the interior of an ellipse onto a circle. Am. Math. Monthly **57**, 474–479 (1950)
26. Trott, M.: The Mathematica GuideBook for Numerics. Springer Science+Business Media, Inc., Berlin (2006)
27. Whittaker, E.T., Watson, G.N.: A Course of Modern Analysis, reprint of the (1927) 4th edition, Cambridge Mathematical Library. Cambridge University Press, Cambridge (1996)
28. Williams, G.B.: A circle packing measurable Riemann theorem. Proc. Am. Math. Soc. **134**, 2139–2146 (2006)